NASA Contractor Report 165965
Final Technical Report FY 1980/1981

Development of Powder Metallurgy Al Alloys for High Temperature Aircraft Structural Applications — Phase II

D.J. Chellman

LOCKHEED-CALIFORNIA COMPANY
BURBANK, CALIFORNIA

CONTACT NO. NAS1-16048
MODIFICATIONS 1 AND 2
NOVEMBER 1982

NASA
National Aeronautics and
Space Administration

Langley Research Center
Hampton Virginia 23665

NASA Contractor Report 165965
Final Technical Report FY 1980/1981

Development of Powder Metallurgy Al Alloys for High Temperature Aircraft Structural Applications — Phase II

D.J. Chellman

LOCKHEED-CALIFORNIA COMPANY
BURBANK, CALIFORNIA

CONTACT NO. NAS1-16048
MODIFICATIONS 1 AND 2
NOVEMBER 1982

National Aeronautics and
Space Administration

Langley Research Center
Hampton Virginia 23665

Page intentionally left blank

Page intentionally left blank

FOREWORD

This report documents the results of an on-going technical assessment for the FY 1980/1981 time period performed by the Lockheed-California Company on advanced powder metallurgy Al alloys. The reporting period is from 16 July 1980 through 15 August 1981. The research study was conducted for the NASA Advanced Supersonic Technology Project Office under NASA Contract NAS1-16048, Modifications 1 and 2. S.M. Dollyhigh and W.B. Lisagor served as Technical Monitors on the present effort at the NASA-Langley Research Center.

M.L. Ochieano was the Lockheed Task Leader and D.J. Chellman was the Lockheed Principal Investigator, with technical support from H.C. Slaughter. G.G. Wald served as consulting Metallurgist. F. Heck and J.A. Walker were Project Leaders for subcontractor work performed by the International Nickel Company (Inco) and Aluminum Company of America (Alcoa), respectively. The author is grateful to W.W. Leuders, R.C. Lal, and P.S. McAuliffe for their helpful contributions to this study. Acknowledgement is also given to the support personnel at Inco and Alcoa for their technical assistance.

NASA Contractor Report 165676 covers the advanced powder metallurgy Al alloy evaluation conducted by the Lockheed-California Company prior to this contract.

Page intentionally left blank

Page intentionally left blank

CONTENTS

CONTENTS (Continued)

LIST OF ILLUSTRATIONS

LIST OF ILLUSTRATIONS (Continued)

LIST OF TABLES

DEVELOPMENT OF POWDER METALLURGY AL ALLOYS FOR HIGH TEMPERATURE AIRCRAFT STRUCTURAL APPLICATIONS – PHASE II

D.J. Chellman

Lockheed-California Company

SUMMARY

This report describes the analytical and test work completed by the Lockheed-California Company during FY 1980/1981 on the exploratory work being conducted on advanced powder metallurgy Al alloys in support of the NASA supersonic cruise research project. The FY 1980/1981 development effort is a continuing study and covers three types of metallurgical systems. The reinforcement of 2XXX series Al alloys with silicon carbide (hereafter referred to as metal matrix composite) was added to the development effort during FY 1980/1981, and is described in a separate technical report. A summary of the research work for two unreinforced Al alloy systems involving mechanical alloying and atomization is given as follows:

Mechanically Alloyed Powder Metallurgy (MAPM)

In this continuing study, the development of mechanically alloyed heat resistant aluminum alloys for aircraft was directed toward higher strength targets and higher service temperatures. The use of higher alloy additions to MA Al-Fe-Co alloys, employment of prealloyed starting materials, and higher extrusion temperatures were investigated. While the MA Al-Fe-Co alloys exhibited good retention of strength and ductility properties at elevated temperatures and excellent stability of properties after 1000 hour exposure at elevated temperatures, a sensitivity of this system to low extrusion strain rates adversely affected the level of strength achieved. MA alloys in the Al-Li family showed excellent notched toughness and property stability after long time exposures at elevated temperatures. A loss of Li during processing (as yet unexplained) and the higher extrusion temperature 482K (900°F) resulted in low mechanical strengths. Subsequent hot and cold working of the MA Al-Li had only a mild influence on properties.

The advantage of using prealloyed powders as a starting material, while producing cleaner structure, could not be clearly established because of the attritor processing anomalies encountered and because of the changes in thermomechanical processing conditions.

Attempts to mechanically alloy the Al-Fe-Ce alloy were unsuccessful. A greater in-depth study of processing parameters will be required to establish appropriate attritor conditions.

MAPM Goal Realization

- The MA Al-Fe-X alloy systems explored so far have not attained the room temperature strength improvements required to effect an aluminum design competitive with a titanium design. FY 1980/1981 work showed no improvement over FY 1979 work relative to attaining ultimate strength. The alloy system has displayed a thermally stable matrix (after 1000 hour exposure) and less than a 25 percent drop in strength at 450K (350°F), the temperature limit of this program.

- The MA Al-Li system displayed a similar behavior to the Al-Fe-X system in that room temperature strength was below target goals (FY 1979 work, Reference 1, indicated a strength greater than the target goal). Thermal exposure up to 1000 hour had negligible effects on strength stability, however this alloy system had a loss in strength at temperature of approximately 50 percent at 450K (350°F).

Powder Metallurgy (PM)

Six powder metallurgy extruded materials were studied during FY 1980/1981. PM 2618 MOD A (high Si, Fe, low Ni), PM 2124 MOD (high Mn) and PM 2124, which were tested and reported in the previous work[1], received follow-on optical, scanning electron microscopy, and pinhole X-ray metallographic evaluations. The Alcoa atomization/compaction/consolidation/extrusion sequence (Figure 4) was used to produce the new test materials; PM Hiduminium (HID) 543 MOD (low Cu), PM 2618, and PM 2618 MOD B (no Fe, Ni). The promise of elevated temperature property improvement based on published and private data was the basis for selecting these three new alloys. Composition, X-ray crystallographic, optical metallographic, and thermomechanical precipitation strengthening studies were conducted for the new materials. Ambient property comparisons were made for the six materials of this project and they were further compared with other ingot and powder metallurgy members of the 2XXX Al alloy family.

PM Goal Realization

- At ambient temperature, the peak-aged ultimate strength of the six percent stretched PM 2618 MOD B (no Fe, Ni) meets the design minimum target value for damage tolerant application; the six percent stretched PM HID 543 MOD (low Cu) and PM 2618 materials approach but do not meet the target value. However, none of those three materials provided ambient strength improvements over conventional ingot metallurgy 2XXX materials to the extent provided by the PM 2124 MOD (high Mn) and PM 2124 alloys introduced earlier in this project. Temperature stability has not yet been tested for the new materials although the body of aging study data suggests that the 2618 alloy PM derivatives may have slightly greater stability than the 2124 PM derivatives.

- The PM HID 543 MOD material showed a marked decline in maximum obtainable strength with increasing aging temperature. PM 2618 and PM 2618 MOD B were more stable and were therefore selected for on-going study. Two step aging did not show a strength gain over single step aging for the PM 2618 candidates. The PM 2618 and PM 2618 MOD B candidates joined the PM 2124 items tested earlier in showing fracture toughness improvements over IM 2124.

- Toughness of the PM 2124 and PM 2124 MOD materials tested earlier decreases with increased dispersoid/constituent content and fractography shows an attendant finer and closer packed dimple distribution on the fracture surfaces.

- Thermal stability, fracture toughness, corrosion resistance, and fatigue resistance are to be concluded for the PM 2618 and PM 2618 MOD B materials in the follow-on activity.

INTRODUCTION

Objectives

The general objective of the supersonic cruise research technology assessment studies is to identify the research and development necessary to support decisions related to plans for future United States commercial air transportation.

This report covers the development effort underway on exploring aluminum powder metallurgy technology and powder metallurgy alloy systems. Aluminum alloys are of interest for higher performance commercial aircraft because of their relatively low cost and ease of fabrication.

The development work reported herein covers distinctly different families of alloys each tailored to satisfy different design requirements. The goals for the specific alloy types are high strength, damage tolerant, high modulus, and low density. The families of alloys are divided into two metallurgical systems of alloying, namely: (1) powder metallurgy (PM) metals, and (2) mechanically alloyed powder metallurgy (MAPM) metals. The powder metallurgy metals are being developed in coordination with Aluminum Company of America (Alcoa). The mechanically alloyed PM metals are being developed in cooperation with International Nickel Company (Inco). The target property goals (Table 1) for the families of Al alloys are basically as previously stated in NASA Contractor Report 165676 which details the FY 1979 work. The table has been modified for FY 1980/1981 work to include target goals for MMC materials. Work approach for this report period included:

Mechanically Alloyed Powder Metallurgy (MAPM)

- Evaluate higher constituent levels to achieve higher strength [579 MPa (84 Ksi)] in the MAPM Al-Fe-X system;

TABLE 1. FOUR CATEGORIES OF TARGET PROPERTIES (1)

REQUIREMENTS	HIGH STRENGTH CORROSION RESISTANCE A		HIGH STRENGTH CORROSION RESISTANCE B		DAMAGE TOLERANCE		HIGH STIFFNESS		LOW DENSITY		HIGH STRENGTH HIGH MODULUS (2)	
1. STRENGTH F_{tu}–MPa (KSI)	579	(84)	517	(75)	479	(68)	427	(62)	427	(62)	586	(85)
F_{cy}–MPa (KSI)	558	(82)	503	(73)	427	(62)	379	(55)	379	(55)	538	(78)
2. FATIGUE: * F_{MAX}–MPa (KSI)	159	(23)	145	(21)	206	(30)	131	(19)	131	(19)	159	(23)
Δ K-MPa $\sqrt{M}$ (KSI $\sqrt{IN}$)	6.2	(6.2)	6.16	(5.6)	7.92	(7.2)	6.16	(5.6)	6.18	(5.6)	6 82	(6 2)
3. FRACTURE TOUGHNESS:												
K_{APP} – MPa $\sqrt{M}$ (KSI $\sqrt{IN}$)	66	(60)	66	(60)	89.1	(81)	66	(60)	66	(60)	66	(60)
K_{IC} – MPa $\sqrt{M}$ (KSI $\sqrt{IN}$)	28.6	(26)	28.6	(26)	33	(30)	28.6	(26)	28.6	(26)	28.6	(26)
4. DENSITY: GRAMS/CM^3 (LB/IN^3)	2 79	(0.101)	2.5	(0.09)	–	–	–	–	2.5	(0.09)	2.79	(0.101)
5. ELASTIC MODULUS: GPa (MSI)	72 5	(10.5)	85.4	(12.4)	73.7	(10.7)	81.4	(11.8)	81.4	(11 8)	108	(15.6)
6. CORROSION RESISTANCE.												
STRESS CORROSION MPa (KSI)	172	(25)	172	(25)	172	(25)	172	(25)	172	(25)	172	(25)
EXFOLIATION CORROSION	>EA		>EA		>EA		>EA		>EA		>EA	
*F_{MAX} AT 10^5 CYCLES, $K_T = 3$, R = 0.1 ΔK FOR R = 0.1, DA/DN ~ 10^{-6} IN/IN												

(1) ELEVATED TEMPERATURE PROPERTIES

- STABILITY – ROOM TEMPERATURE PROPERTIES UNAFFECTED
- GREATER THAN 80 PERCENT OF ROOM TEMPERATURE

(2) 5 PERCENT ELONGATION SET AS TARGET GOAL

- Explore potential of MAPM Al-1.7 Li alloy using prealloyed powder;
- Determine effects of higher temperatures in extruding MAPM alloys;
- Determine elevated temperature strengths and stability of MAPM alloys up to 450K (350°F).

Powder Metallurgy (PM)

- Prepare one each PM HID 543 MOD (low Cu), PM 2618, and PM 2618 MOD B (no Fe, Ni) alloy in extruded bar form;
- Conduct stretch and age study for smooth and notched tensile screening tests, and select the two most promising alloys;
- Conclude metallographic studies attendant to determination of matched fracture toughness and fatigue resistance of PM 2618 MOD A (high Si, Fe, low Ni), PM 2124 MOD (high Mn), and PM 2124 extrusions;
- Determine the effect of fine intermetallic particles on notched fatigue resistance in naturally and artificially aged tempers for the PM 2618 variant;
- Compare the two most promising new materials with PM 2618 MOD A (high Si, Fe, low Ni), PM 2124 MOD (high Mn), PM 2124 alloys tested previously, and with other 2XXX IM and PM materials in various product forms.

Background

Mechanically Alloyed Powder Metallurgy (MAPM)

The mechanical alloying approach is designed to achieve high strength with a fine dispersion of stable strengthening particles in an otherwise homogeneous microstructure. Strength at elevated temperature is also improved by a metallurgically stable structure. Such a dispersion inhibits dislocation motion and thereby improves creep resistance.

The mechanical alloying process is a technique for producing composite metal powders with controlled fine microstructures. It occurs by the fracturing and rewelding of a mixture of powder particles during milling via a highly energetic ball charge. The process takes place entirely in the solid state.

The repetitive cold welding and fracturing of the powder particles during mechanical alloying of aluminum incorporates the naturally occurring oxides on the surface of the powder particles into the interior of the composite powder particles. As the process continues with repetitive welding and fracturing of the powder particles, the incorporated oxide particles are

reduced in size as they are homogeneously dispersed throughout the composite powder particles. In a similar fashion, metallic alloying ingredients also are thoroughly distributed within the powder particles. The fineness of the dispersion of both the oxide and metallic ingredients achieved by the mechanical alloying process leads to the superior properties of mechanically alloyed materials.

Powder Metallurgy (PM)

An exploratory program to develop high strength, damage tolerant PM 2XXX alloys with elevated temperature stability has shown that the powder metallurgy approach can improve the mechanical properties of 2124 and 2618 alloys over that of their IM counterparts[1]. The program revealed that the fracture toughness of a high Cu 2618 composition is lower than one based on 2124. This is likely due to a higher volume fraction of insoluble second phase caused by the high Cu level and the increased additions of Fe and Ni over that commonly used in 2618.

Examination of the ternary phase diagram shows that the highest copper content for a 1.6 wt. pct. Mg alloy still in a single phase field at 773K (932°F) is 3.5 wt. pct.[2]. Prior work at Alcoa also has shown that maximum strength at 422K (300°F) occurs at this copper content. This behavior suggests that the alloy with the optimum elevated temperature strength should have the highest solute content, keeping within the limit of solid solubility.

The addition of Fe and Ni to the IM 2618 alloy is justified by its improvement in creep resistance[3]; however, the PM alloy has naturally occurring oxides which are potent grain structure stabilizers. These oxides may accomplish in the PM alloy the same results that the $FeNiAl_9$ dispersoid does in the IM alloy. It, therefore, seems highly useful to examine the room and elevated temperature tensile properties and the fracture toughness of a PM analogue containing $\lesssim 3.5$ wt. pct. Cu (at approximately 1.6 wt. pct. Mg) with no Fe and Ni additions.

A pertinent area of PM alloy design is the unexamined Al-Cu compositions strengthened by θ', θ'', or GP zones. Alloys based on Al-Cu, with and without trace element additives, merit study since their thermal stability in terms of strength is generally better than alloys containing the S phase. Addition of a trace element improves the thermal stability and possibly the strength of the Al-Cu alloy by controlling the nucleation density and/or coarsening behavior of hardening precipitates. It is possible that the additions may accelerate or retard the early stages of zone formation so that the normal sequence of precipitation events is altered. The stability after long-term exposures can be the same as, or lower than, that of a comparable trace element free alloy[4]. By the use of PM techniques, an increase in room temperature strength due to structure refinement, similar to that observed in PM 2024, may be obtained in Al-Cu alloys.

SYMBOLS, ABBREVIATIONS, AND ACRONYMS

SYMBOL	DEFINITION	SI UNITS	CUSTOMARY ENGINEERING UNITS
AA	Artificially Aged	-	-
E_c	Modulus of Elasticity in Compression	GPa	MSI
E, E_t	Modulus of Elasticity in Tension	GPa	MSI
ε	Engineering Strain	m/m	in/in
$\bar{\varepsilon}$	Effective Extrusion Strain	non-dim	non-dim
$\dot{\varepsilon}$	Time-Average Strain Rate	mm/mm-sec	in/in-sec
G.P. (B) Zones	Pre-Precipitation Clusters of Cu Atoms on Al Cube Planes	-	-
Hi-Cu	High Copper	-	-
Hi-Mn	High Manganese	-	-
hr	Hour	-	-
HM	High Elastic Modulus	-	-
HS	High Strength	-	-
ΔK	Stress Intensity Factor Range	MPa-$m^{\frac{1}{2}}$	ksi-$in^{\frac{1}{2}}$
K_{app}	Apparent Plane Stress Fracture Toughness	MPa-$m^{\frac{1}{2}}$	ksi-$in^{\frac{1}{2}}$
K_c	Critical Stress Intensity Factor	MPa-$m^{\frac{1}{2}}$	ksi-$in^{\frac{1}{2}}$
K_{SC}	Stress Concentration Factor	-	-
MA	Mechanically Alloyed	-	-
MMC	Metal Matrix Composite	-	-
NA	Naturally Aged	-	-
NTS	Notched Tensile Strength	MPa	ksi
NTS/YS	Notched Tensile Strength to Yield Strength Ratio	non-dim	non-dim
R	Minimum to Maximum Fatigue Stress Factor	-	-
ρ	Density	MPa/m	lb/in^3

SYMBOL	DEFINITION	SI UNITS	CUSTOMARY ENGINEERING UNITS
SEM	Scanning Electron Microscopy	-	-
SHT, ST	Solution Heat Treatment	-	-
σ	Engineering Stress	MPa	ksi
s, sec	Seconds	-	-
S	Al_2CuMg Intermetallic Precipitate Equilibrium Phase	-	-
S'	Al/Cu/Mg Transition Phase	-	-
SiC_w	Silicon Carbide Whiskers	-	-
SiC_p	Silicon Carbide Particulates	-	-
θ	Al_2Cu Intermetallic Precipitate Equilibrium Phase	-	-
θ'	Al/Cu Transition Phase	-	-
θ''	Ordered 2nd Step G.P. Zone Formation (G.P. II)	-	-
TMT	Thermomechanical Treatment	-	-
WQ	Water Quench	-	-
w/o, wt. pct.	Weight Percent	-	-
YS	Yield Strength (0.2% Offset)	MPa	ksi

PROCEDURE

Material Selection

Mechanically Alloyed Powder Metallurgy (MAPM)

The mechanical alloying (Inco developed) study was conducted by Inco Research and Development Center (IRDC). In the work completed in 1979[1], Inco evaluated thirteen MAPM alloys involving Al-Fe-X and Al-Li systems. Alloys in the Al-Fe-X system exhibited good potential for use as damage tolerant-fatigue resistant alloys, while alloys in the Al-Li family showed promise as high stiffness-low density materials. The work reported herein is a continuation of this effort wherein further exploratory work was conducted to provide compositions of the Al-Fe-X and Al-Li systems.

A total of five alloy lots were to be prepared. The nominal compositions of the planned materials, the dispersoid level, and the extrusion conditions are given in Table 2. To achieve as complete processing as possible, prealloyed powders were used as starting materials when feasible. For the Al-Fe-Co system, a prealloyed Al-3Fe powder was blended with elemental Al and Co powders to obtain the desired composition. An Al-Fe-Ce master alloy of the desired composition was prepared by IRDC and subsequently atomized at Valimet, Inc., Stockton, California and returned to IRDC as prealloyed powder for attritor processing. A nominal Al-1.7Li prealloyed powder was produced at Homogeneous Metals, Inc., Herkimer, New York and sent to IRDC for processing. Chemical analysis of these prealloyed powders, after receipt of IRDC, are given in Table 2. Typical structures of the prealloyed Al-3Fe and Al-1.7Li powders are shown in Figures 1 and 2.

The size distributions of Lots 1, 2, 5, and 5A attrited powders (Table 2) show significant differences in distribution. The planned Al-Li Lot 5 was extremely coarse as produced in the attritor. On IRDC's recommendation, a second Al-Li lot (designated Lot 5A) was produced to the same composition but at a higher dispersoid level to reduce the coarseness. While considerably finer than Lot 5, the new Lot 5A is still coarser than the Al-Fe-Co alloys (Lots 1 and 2). The inclusion of this Lot 5A permitted the evaluation of the Al-Li system at two dispersoid levels. Chemical analyses of the attrited powders are given in Table 2. Figures 1 and 2 show the structures of these attrited powders.

Powder Metallurgy (PM)

The Al alloys selected are based on the compositions of HID 543[4] and 2618. The HID 543 composition, a low Cu 2219 alloy with approximately 0.3 wt. pct. Mg, offers a potentially excellent combination of room temperature strength and elevated temperature properties[4]. Two alloys are based on the 2618 composition with a higher Cu target composition, 3.5 wt. pct., to improve the elevated temperature properties[5]. One of the high Cu 2618 type alloys did not contain Fe and Ni additions. The Ni and Fe constituents were omitted to determine the effect of the dispersoid on damage tolerance and elevated temperature stability. The Si content, where optimum influence on tensile properties is expected, is approximately 0.20 wt. pct.[6].

Target and actual compositions are listed in Figure 3 (left, second box down). The Cu/Mg ratios indicate that the actual powder compositions are close to the desired value for $Al_2Cu(\theta)$ and $Al_2CuMg(S)$ precipitating alloys, Figure 3 (left, top box). Magnesium losses from the melt due to MgO formation during atomization are compensated for by increasing the melt composition by 0.3 wt. pct. The dispersoid forming elements, Mn, Fe, and Ni, are within acceptable limits. The variation of Si content between PM 2618 and PM 2618 MOD B is higher than originally desired.

TABLE 2. MA TARGET AND ACTUAL COMPOSITIONS, AND EXTRUSION TEMPERATURES

	INGREDIENT IDENTITY OR LOT NO	SOURCE	Li	Fe	Co	O	C	Ce	DISPERSOID	Al	EXTRUSION TEMP TARGET K	EXTRUSION TEMP TARGET (°F)	EXTRUSION TEMP ACTUAL K	EXTRUSION TEMP ACTUAL (°F)
PREALLOYED POWDER (ACTUAL)	Al-3Fe	ALCAN	–	2 9	–	ND	ND	–	–	BAL	–	–	–	–
	Al-Fe-Ce	VALIMET	–	7 8	–	0 42	0 005	–	–	BAL.	–	–	–	–
	Al-Li	HOMOG METALS	1 79	–	–	0 18	0 05	–	–	BAL.	–	–	–	–
BAR (TARGET)	1	–	–	4 9	5.2	–	–	–	4–6	BAL	700	(800)	–	–
	2	–	–	4 9	5 2	–	–	–	4–6	BAL	755	(900)	–	–
	3	–	–	8 1	–	–	–	3 9	4–6	BAL	700	(800)	–	–
	4	–	–	8 1	–	–	–	3 9	4–6	BAL	755	(900)	–	–
	5	–	1 7	–	–	–	–	–	2–3	BAL	755	(900)	–	–
BLEND/BILLET (ACTUAL)*	1 & 2	–	–	4 1	5.1	0 47	0 74	–	4 11	BAL	–	–	–	–
	5	–	1 77	–	–	0 13	0 43	–	2.17	BAL	–	–	–	–
	5A	–	1 76	–	–	0 27	0 80	–	4 07	BAL	–	–	–	–
BAR (ACTUAL)	1	–	–	4 1	5 1	0 46	0 76	–	4 19	BAL	–	–	700	(800)
	2	–	–	4 1	5 0	0 48	0 76	–	4.22	BAL	–	–	755	(900)
	5	–	1 4	–	–	0 18	0 42	–	2 20	BAL	–	–	755	(900)
	5A	–	1 4	–	–	0 41	0 78	–	4 20	BAL	–	–	755	(900)

*SIZE DISTRIBUTION

ALLOY LOT NO.	Al-Fe-Co 1 & 2*	Al-Li 5	Al-Li 5A
SCREEN ANALYSIS (Wt. %)			
+ 10 MESH	–	6.1	0.3
-10 + 20 MESH	–	51.9	4.6
-20 + 30 MESH	–	23.0	4.4
-30 + 45 MESH	0.1	10.6	17.8
-45 + 60 MESH	0.2	3.8	18.0
-60 + 100 MESH	1.3	3.1	42.8
-100 + 200 MESH	5.5	1.1	10.5
-200 + 325 MESH	7.5	0.2	0.9
-325 MESH	85.4	0.2	0.7

*REPRESENTS MATERIAL FOR TWO EXTRUSION RUNS

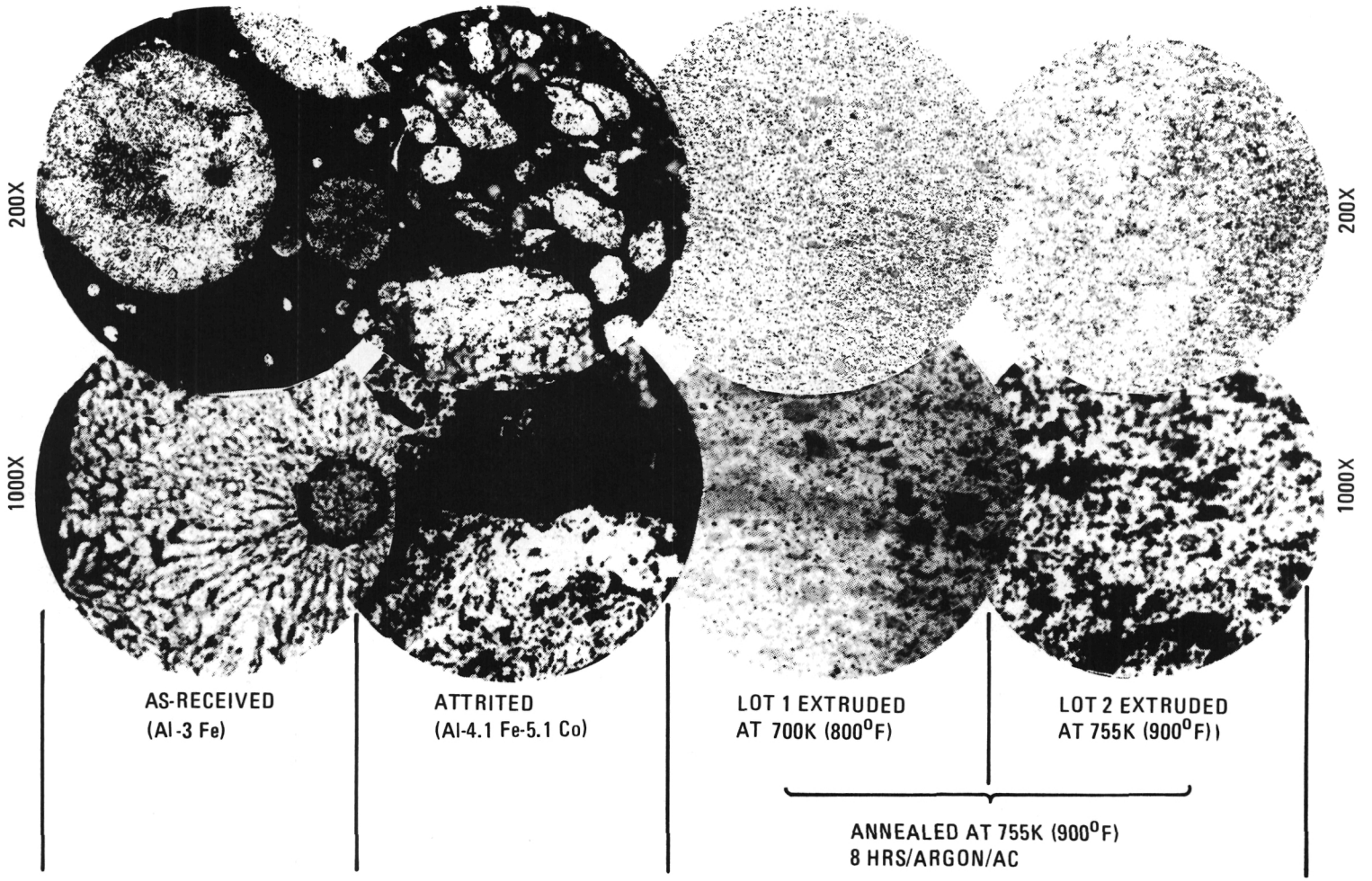

Figure 1. – Progression from ingredient powder through attrited blend (billet metallographic structure not shown) to MA Al - 4.1 Fe - 5.1 Co extrusions.

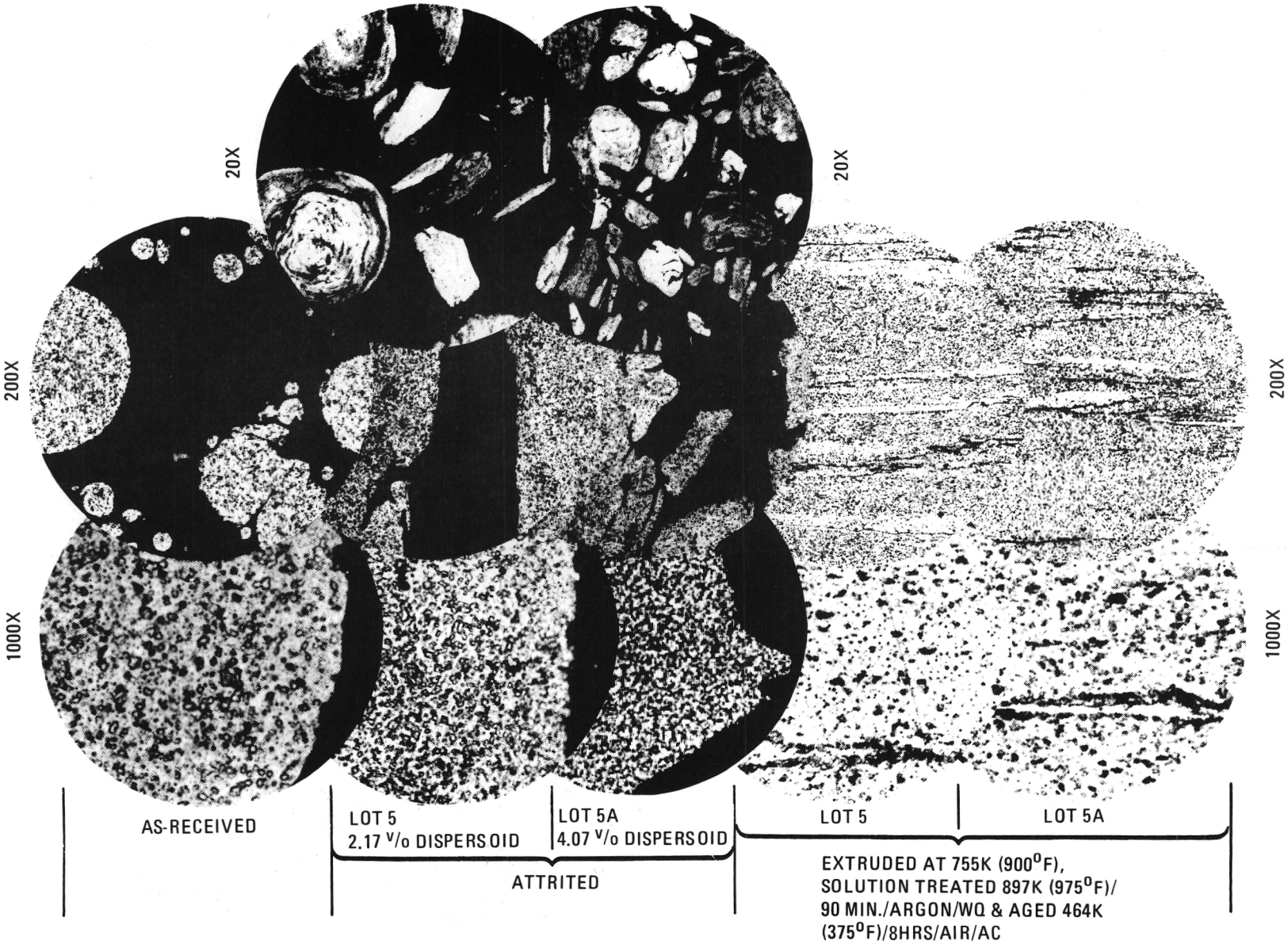

Figure 2. – Progression from ingredient powder through attrited blends (billet macro/micro structure not shown) to MA Al - 1.7 Li extrusions.

POWDER

LIQUID/SOLID TRANSITION CHEMISTRY

GUINIER-deWOLFF X-RAY ANALYSIS OF THE ATOMIZED POWDER

S. NO.	PHASES PRESENT $CuAl_2$	$CuMgAl_2$	Mg_2Si
PM HID 543 MOD	MEDIUM	*	*
PM 2628	POSS. V. SMALL –	*	V. SMALL –
PM 2618 MOD	SMALL	SMALL –	V. SMALL+

*POSSIBLE IS AN UNDETECTABLE AMOUNT

PM 2XXX ALLOY POWDER COMPOSITIONS

ALLOY		Cu	Mg	Mn	Si	Fe	Ni	Ti	Al	Cu/Mg
PM HID 543 MOD (LOW Cu)	TARGET	5.50	0.35	0.30	–	–	–	–	BAL	15.70
	ACTUAL	5.30	0.38	0.20	0.12	0.06	–	0.04	BAL	13.90
PM 2618	TARGET	3.50	1.65	–	0.20	1.20	1.10	–	BAL	2.12
	ACTUAL	3.40	1.53	0.01	0.08	0.98	0.83	0.10	BAL	2.22
PM 2618 MOD B (NO Fe, Ni)	TARGET	3.50	1.65	–	0.20	–	–	–	BAL	2.12
	ACTUAL	3.26	1.69	0.01	0.30	0.10	–	0.08	BAL	1.93
PM 2618 MOD A (HIGH Si, Fe, LOW Ni)	TARGET	3.80	1.80	–	1.50	1.50	0.07	0.10	BAL	–
	ACTUAL	3.87	1.93	0.01	1.53	1.73	0.07	0.07	BAL	2.01
PM 2124 MOD (HIGH Mn)	TARGET	4.00	1.60	1.50	–	–	–	–	BAL	–
	ACTUAL	3.93	1.57	1.50	0.06	0.01	0.00	0.06	BAL	2.50
PM 2124	TARGET	4.00	1.60	0.50	–	–	–	–	BAL	–
	ACTUAL	4.06	1.62	0.51	0.05	0.00	0.00	0.05	BAL	2.47
2124	MAX	4.90	1.80	0.90	0.30	–	0.15	0.20		
	MIN	3.80	1.20	0.30	–	–	–	–		
2618	MAX	2.70	1.80	–	0.25	1.30	1.20	0.10		
	MIN	1.90	1.30	–	0.10	0.90	0.90	0.04		
2219	MAX	6.80	0.02	0.40	–	0.30	0.20	0.10		
	MIN	5.80	–	0.20	–	–	–	0.02		
HID 543		6.00	0.35	0.20	–	–	–	–		

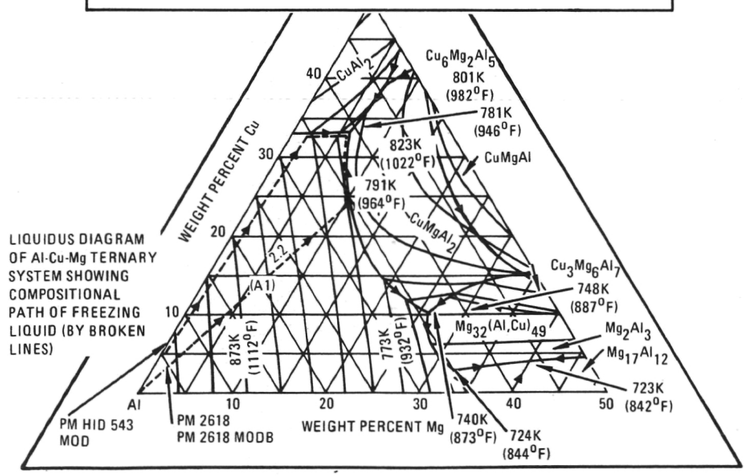

LIQUIDUS DIAGRAM OF Al-Cu-Mg TERNARY SYSTEM SHOWING COMPOSITIONAL PATH OF FREEZING LIQUID (BY BROKEN LINES)

PARTICLE SIZE AND DISTRIBUTION

ATOMIZED POWDER PARAMETERS

ALLOY	SCREEN ANALYSIS (%) -100+200	-200+325	-325	A.P.D.(μm)
PM HID 543 MOD	1.6	4.6	93.6	14.1
PM 2618	1.8	5.2	92.9	13.2
PM 2618 MOD B	3.0	6.6	90.4	13.8
PM 2618 MOD A	1.2	4.6	94.0	11.0
PM 2618 MOD	0.4	2.6	96.8	11.6
PM 2124	2.8	6.6	90.5	12.1

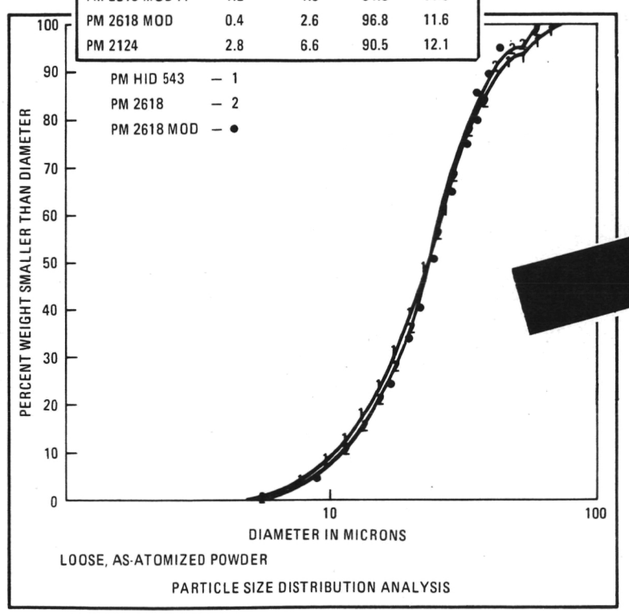

BILLET/EXTRUSION THERMOCHEMICAL BEHAVIOR

THE CALCULATED Cu AND Mg AVAILABLE FOR PRECIPITATION AFTER THE FORMATION OF INSOLUBLE INTERMETALLIC PARTICLES FROM REFERENCE 4.

ALLOY	1 $Al_{20}Mn_3Cu_2$	2 Al_7Cu_2Fe	AVAILABLE Cu	3 Mg_2Si[3]	AVAILABLE Mg	YIELD* STRENGTH MPa (KSI)	Cu	Mg	Mn	Fe	Si	Ni
PM 2618 MOD A	–	1.740	2.130	0.035	1.890	384 (55.7)	3.87	1.93	0.01	1.53	0.07	1.73
PM 2124 MOD	1.001	0.137	2.790	0.017	1.550	453 (65.7)	3.93	1.57	1.50	0.06	0.06	–
PM 2124	0.239	0.114	3.707	–	1.620	456 (66.1)	4.06	1.62	0.51	0.05	0.05	–
PM HID 543 MOD	0.139	0.137	5.024	0.121	0.259	384 (55.7)	5.30	0.38	0.20	0.06	0.12	–
PM 2618	–	1.117	2.283	0.052	1.478	415 (60.1)	3.40	1.53	0.01	0.98	0.08	0.83
PM 2618 MOD B	–	0.114	3.150	0.433	1.257	426 (61.8)	3.26	1.69	0.01	0.10	0.30	–

AGING CONDITIONS FOR ALLOYS (PEAK STRENGTH)	ALLOY	AGING CONDITION ON T351
	PM 2618 MOD A	8 HRS AT 450K (350°F)
	PM 2124 MOD	12 HRS AT 450K (350°F)
	PM 2124	12 HRS AT 450K (350°F)
	PM HID 543 MOD	16 HRS AT 436K (325°F)
	PM 2618	16 HRS AT 450K (350°F)
	PM 2618 MOD B	16 HRS AT 450K (350°F)

1 ASSUMES 0.20 SOLUBILITY OF Mn AT 766K (920°F)
2 ASSUMES 0.00 SOLUBILITY OF Fe AT 766K (920°F)
3 ASSUMES 0.05 SOLUBILITY OF Si AT 766K (920°F)

GUINIER ANALYSIS OF THE HOT COMPACTED PM BILLET

S-NO.	ALLOY	$CuAl_2$ θ	Al_7Cu_2Fe β(Al-Cu-Fe)	Mg_2Si	$FeNiAl_9$	Al_2CuMg S	S'
513887-1	HID 543	V. LARGE	V. SMALL	POSS. TRACE	–	*	–
513887-2	HID 543	V. LARGE	V. SMALL	POSS. TRACE	–	–	–
513888-1	2618	MED.	MED. +	V. SMALL –	MED	SMALL +	–
513888-2	2618	MED.	MED. +	V. SMALL –	MED.	SMALL +	–
513889-1	2618 (NO Fe OR Ni)	LARGE	SMALL	MED.	–	V. SMALL	POSS. TRACE
513889-2	2618 (NO Fe OR Ni)	LARGE	SMALL	MED.	–	V. SMALL	–

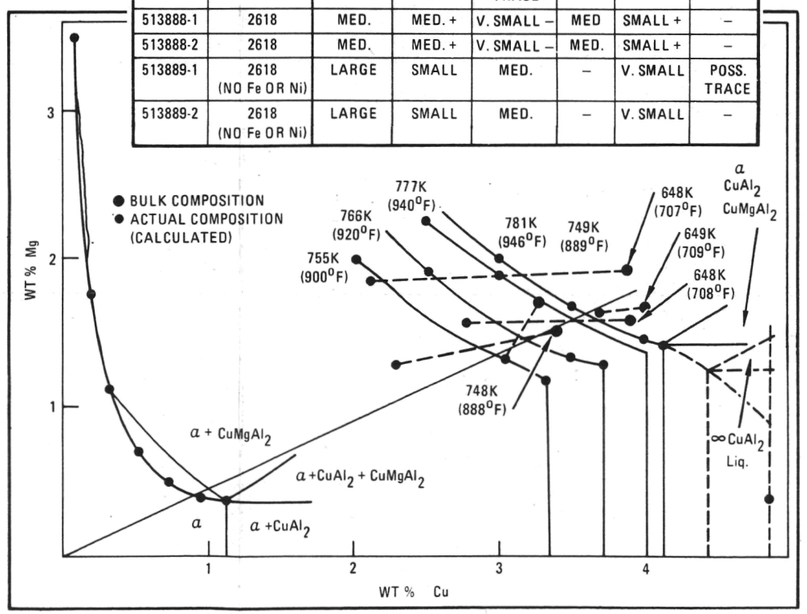

Figure 3. – Library of PM ingredient and test material composition data.

Page Intentionally Left Blank

Approximately 300 pounds of irregularly shaped powder was obtained for each composition. Figure 3 (top center) lists the U.S. standard screen analysis and the average particle diameter determined by a Fisher subsieve sizer. Together with the particle size distribution depicted in Figure 3 (lower center), the results indicate that the solidification rate each alloy powder lot experienced during atomization was similar.

Powder Microstructures.- The fine, mostly dendritic, structure of the irregularly shaped powder particles is shown in Figure 4. The one to three micrometer dendrite arm spacing indicates that cooling rates from 10^3 to 10^5 K/sec are experienced during atomization. A finer dendritic structure is observed in PM 2618 MOD B as a consequence of Fe and Ni additions to the base alloy. Cellular structures indicative of a substantially higher undercooling are occasionally observed.

Figure 3 (left, upper) lists the phases identified by Guinier phase analysis in the as-atomized powders. The volume fraction of each phase is ranked semi-quantitatively by comparing the line intensity of a test film to that of a standard.

The presence of Al_2Cu detected in the three alloys is a result of solute segregation which creates the cored, mostly dendritic, structure in Figure 4. During solidification, solute is rejected from the solid, thereby progressively increasing the liquid solute content. The changing compositional path of the freezing liquid is depicted by the liquidus diagram in Figure 3 (left, bottom). For alloys with Cu/Mg ratios greater than and less than 2.2:1, the freezing liquid follows the path to the left and right of the quasi-binary hump, respectively,

$$Al_{\text{solid solution}} + Al_2Cu + Al_2CuMg.$$

If the solidification rate is sufficiently high the solute can be retained in metastable, supersaturated solid solution. At lower solidification rates Al_2CuMg, Al_2Cu, and Mg_2Si may precipitate during the cool-down to ambient temperatures after the last liquid solidified at the eutectic composition. Rapid age hardening occurs due to the high concentration of quenched-in vacancies promoting rapid diffusion[7].

Rapid quenching can completely eliminate detrimental constituent particles by suppressing the primary crystallization of the complex intermetallic phase. With higher levels or slower, but still rapid, solidification rates, the attendant suppression can lead to the crystallization of the primary intermetallic phase as an array of very fine dispersoid particles. This arrangement

of the intermetallic phase is a highly desirable one. It serves to strengthen the alloy as well as provide stability to the grain size and substructure. In summary, rapid solidification technology benefits elevated temperature aluminum alloy development by providing a starting material with a very fine microstructure that is supersaturated with alloying elements, free of constituent particles, and can contain very fine dispersoid particles. The vast area of grain boundaries that exists in a fine grained material serves as a very effective impediment to dislocation motion, thereby inducing alloy strengthening. The presence of solute atoms in solid solution impedes dislocation mobility, not only by lattice distortion, but also by serving to "roughen" the slip planes. This combined resistance to the movement of dislocations represents an increment of added strength for the alloy. Furthermore, hardening is obtained when precipitates or dispersoids are very strong and closely spaced. This represents the mechanism of dispersion strengthening.

The amount of Al_2CuMg detected, Figure 3 (lower right), is much less than expected for the bulk composition of PM 2618 and PM 2618 MOD B. Eutectic segregation creates solute-rich regions around the periphery of the dendrite arms. The relative abundance of Al_2Cu indicates that the local Cu/Mg ratio within high solute regions of the segregated powder must be at least 8:1. Constituent phases which contain Fe, Ni, and Mn were not detected by Guinier analysis or observed in the as-polished powders at 1000X.

Materials and Specimen Preparation

Mechanically Alloyed Powder Metallurgy (MAPM)

Several attempts were made to mechanically alloy the Al-Fe-Ce alloys (Lots 3 and 4). All attempts were unsuccessful. Substantial grinding occurred during the attriting process with the result that the powders obtained were either highly pyrophoric in nature or severely packed on the attritor bottom as a consequence of inadequate processing. The quantity of prealloyed Al-Fe-Ce powder received was insufficient to permit the prolonged investigations necessary to define mechanical alloying processing conditions. The remaining unused powder (approximately eight pounds) was sent to Professor N.J. Grant at the Massachusetts Institute of Technology (MIT) for extrusion evaluation.

Prior to canning, the attrited Al-Fe-Co alloys (Lots 1 and 2) were screened to -45 mesh. Because of powder coarseness, Lot 5 (Al-Li) was canned as -10 mesh powder while Lot 5A was screened to -30 mesh. The sieved powders were placed in 11.4 cm (4.5 in.) O.D. x 0.64 cm (.25 in.) wall x 30.5 cm (12 in.) long aluminum alloy 6061 extrusion cans. The cans were then welded closed, except for a .95 cm (.375 in.) diameter evacuation tube (see Figure 5).

Degassing was accomplished in two stages using vacuum evacuation. All cans were evacuated at room temperature to a pump pressure of < 50 μm. They were subsequently placed in furnaces set at 784K (950°F) and held until the pump pressure was again below about 25-50 μm. This degassing of the heated

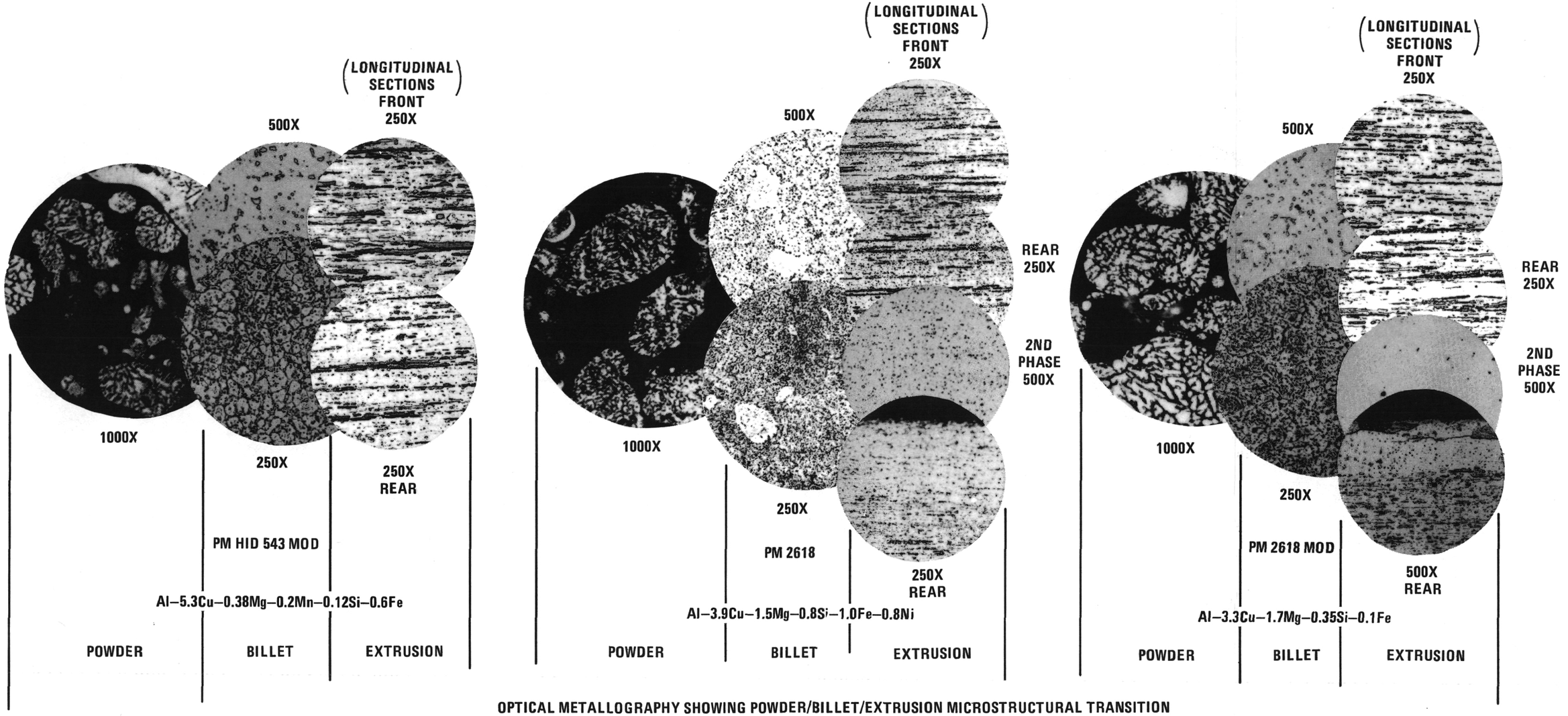

OPTICAL METALLOGRAPHY SHOWING POWDER/BILLET/EXTRUSION MICROSTRUCTURAL TRANSITION FOR 2XXX TYPE TEST MATERIALS

Figure 4. – Optical metallography showing powder/billet/extrusion microstructural transition for 2XXX type test materials.

Page Intentionally Left Blank

EXTRUSION ANALYSIS RESULTS									
LOT NO.	COMPOSITION	EXTRUSION TEMP. K	EXTRUSION TEMP. (°F)	EFFECTIVE STRAIN	TIME AVERAGED STRAIN RATE sec^{-1}	EXTRUSION CONSTANTS AT BREAK-THROUGH MPa	AT BREAK-THROUGH (ksi)	MINIMUM MPa	MINIMUM (ksi)
1	Al-Fe-Co	700	(800)	3.05	0.71	144.8	(21.0)	140.0	(20.3)
2	Al-Fe-Co	755	(900)	3.04	1.03	128.2	(18.6)	125.5	(18.2)
5	Al-Li	755	(900)	3.05	1.11	89.6	(13.0)	88.3	(12.8)
5A	Al-Li	755	(900)	3.05	1.19	64.8	(9.4)	64.1	(9.3)

EXTRUSION CONDITIONS FOR ATTRITED ALLOYS				
	Al-Fe-Co		Al-Li	
ALLOY LOT NO.	700	2	5	5A
EXTRUSION TEMPERATURE, K (°F)	427 (800)	755 (900)	755 (900)	755 (900)
SOAK TIME, hours	3	3	3	3
THROTTLE SETTING, %	30	30	30	30
EXTRUDED BAR SIZE: WIDTH, cm. (in.)	2.87 (1.29	2.86 (1.126)	2.85 (1.124)	2.86 (1.126)
HEIGHT, cm. (in.)	1.80 (0.708	1.81 (0.712)	1.80 (0.710)	1.80 (0.707)
AVERAGE RAM SPEED, cm./sec. (in./sec.)	0.46 (0.18)	0.66 (0.26)	0.71 (0.28)	0.76 (0.30)
EXTRUSION RATIO	21.0	21.0	21.0	21.1

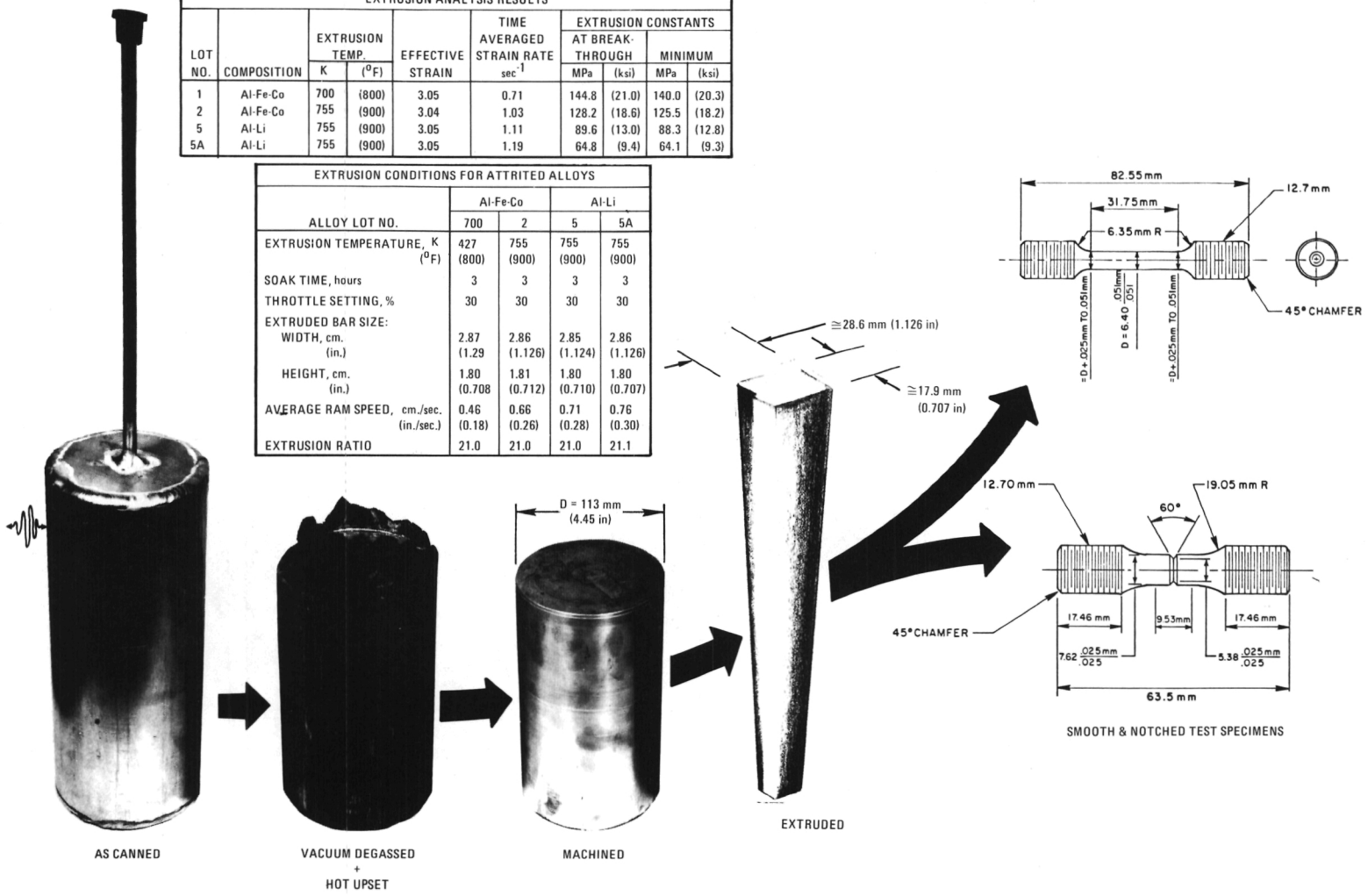

Figure 5. – Test material and specimen preparation sequence.

powder required between 3 and 4-1/2 hours. The cans were subsequently crimp sealed with the vacuum pump still attached to the evacuation tube.

Compaction, performed immediately after sealing, utilized a blank die in a 6.67 MN (750 ton) extrusion press. The maximum pressure of approximately 1000 MPa (145 ksi) was applied for 20 seconds. The compacted billets were lathe-turned to 11.3 cm (4.45 in.) diameter prior to extrusion.

The extrusion conditions for the four alloys are given in Figure 5. All billets were soaked for three hours prior to extrusion. All billets were extruded at either 700K (800°F) or 755K (900°F). Throttle settings of approximately 30 percent were used to produce the nominal 2.86 cm (1.125 in.) x 1.78 cm (0.7 in.) rectangular bars. The temperature-extrusion ratio (21:1) combination yielded ram speeds between 0.46 and 0.76 cm/sec (0.18 to 0.30 in/sec). All extruded bar appeared sound, free from cracking and blistering. Nose and tail defects were removed prior to evaluation. Figure 5 shows typical billets after canning and prior to vacuum degassing, after hot upsetting and after machining prior to extrusion.

The alloy bars produced for this program were given either an annealing treatment (Al-Fe-Co alloys) or a solution plus age treatment (Al-Li alloys) prior to evaluation of mechanical properties. The Al-Fe-Co alloys were given the same annealing treatment, 755K (900°F) + AC and 839K (1050°F) + AC, as outlined in the previous study[1]. For the Al-Li alloys, solution temperatures of 797K (975°F) and 852K (1075°F) were examined. The effect of time (up to 72 hr) on hardness was determined using an aging temperature of 464K (375°F).

The influence of a small amount of hot rolling on the Al-Li alloys was examined as a means of improving material ductility without seriously decreasing strength. Samples were hot rolled approximately 25 percent from 755K (900°F) (the as-extruded temperature) in two passes to a nominal thickness of 1.27 cm (0.50 in.). Based on a study by Jones and Das[9], the effect of an intermediate cold rolling sequence on the Al-Li alloys was examined. Following solution treatment, samples of the Al-Li alloys were immediately cold rolled approximately 25 percent in two passes to a nominal thickness of 1.27 cm (0.50 in.) and then aged.

The trends observed in the MA Al-Fe-X systems during an earlier study[1] suggested that higher strength levels could be expected in these alloys by an increase in alloy content. Two alloys in this system were chosen for evaluation at a five atomic percent addition (a nearly three-fold increase over the nominal 1.7 atomic percent additions previously evaluated). Unforeseen difficulties arising during the attritor processing of a chosen Al-Fe-Ce alloy prevented any evaluations of this alloy. The behavior of this alloy during processing indicated the need for a greater in-depth study beyond the scope of this program.

Chemical analyses of MAPM extruded bar material is shown in Table 2. While the alloy contents of the MA Al-Fe-Co alloys (Lots 1 and 2) closely compare to those of the attrited powders, the MA Al-Li alloys (Lots 5 and 5A) exhibit a substantial loss in Li levels. This 20 percent decrease in Li

content is unusual, particularly since a prealloyed Al-Li starting material was employed, and was not observed in the previous study (where elemental Al and Li powders were used). Processing techniques used for canning, vacuum degassing, and hot upsetting were the same as used in the previous study. Nothing in the recorded processing procedures readily accounts for this loss. Samples of extruded Lots 5 and 5A re-examined at Lockheed showed Li levels of 0.96 and 0.93, respectively, a further decrease from those observed at IRDC. Until this anomaly is resolved, it must be assumed that the Li level of these MA Al-Li alloys is in the range of 1.0 - 1.4 weight percent instead of 1.7 weight percent.

Analysis of the extrusion behavior of these materials included calculations of effective extrusion strain, time-average strain rate, and extrusion constraints. The analysis is based on the same principles discussed in the previous study[1].

The similarity of effective strains, see Figure 5, was expected since all bars were extruded to the same nominal size, 2.86 cm x 1.78 cm (1.125 in. x 0.70 in.). The extrusion strain rates are of the order that would be expected when extruding aluminum alloys at the speeds employed. At a constant throttle setting, the effect of lower extrusion temperature on decreasing the strain rate was demonstrated with the Al-Fe-Co alloys.

The results of the extrusion constant determinations are given in Figure 5. Two "constants" are provided - the constants corresponding to breakthrough and the minimum extrusion pressure. The extrusion process at breakthrough is a transient condition which is highly dependent on the die parameters, among other factors. The constants at breakthrough are thus provided for informational purposes and will not be discussed further except to note that they are higher than the values obtained during the bar extrusion stage.

The "minimum" extrusion constants represent the effective resistance of the billet material to deformation. The constants increase with decreasing extrusion temperature. The constants also decrease with increasing dispersoid level. The experimental extrusion parameters determined are somewhat lower than those previously reported[1] and reflect the effect of lower extrusion ratio and increased billet size.

The results of the solution heat treatments and aging exposures on the hardness of the Al-Li alloys (Lots 5 and 5A) are shown in Figure 6. The hardness levels obtained were considerably lower than those previously observed and are possibly due to a combination of higher extrusion temperature, lower volume percent dispersoid, starting material, and alloy content. Based on this study, the selected heat treatment for the Al-Li alloys was:

797K (975°F)/90 min/Argon/WQ plus 464K (375°F)/8 hours/Air/AC.

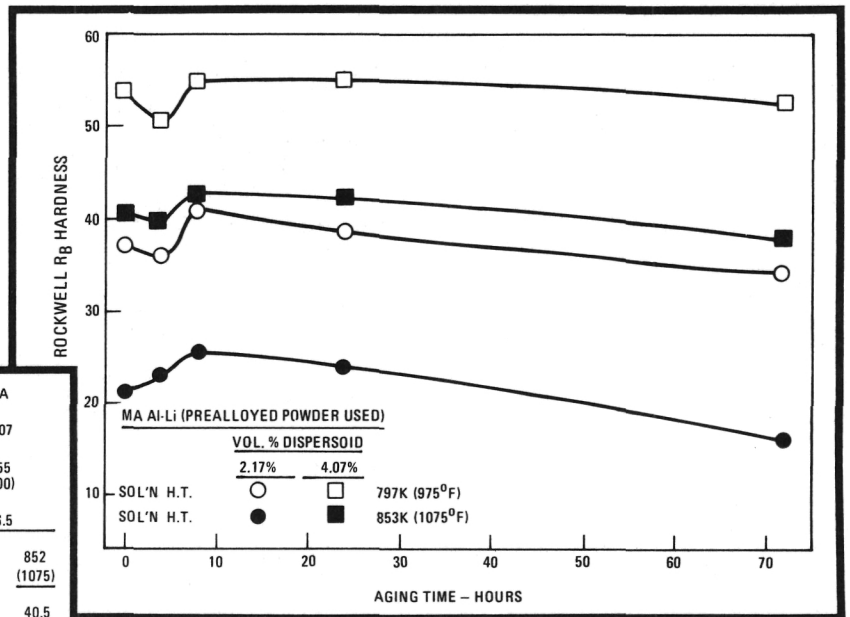

LOT. NO.	5		5A	
VOLUME % DISPERSOID	2.17		4.07	
EXTRUSION TEMPERATURE, K (°F)	755 (900)		755 (900)	
R_B HARDNESS – AS EXTRUDED	40.0		56.5	
SOLUTION TEMPERATURE, K (°F)	797 (975)	852 (1075)	797 (975)	852 (1075)
R_B HARDNESS – AS SOLUTION TREATED	37.5	21.5	54.0	40.5
R_B HARDNESS AS SOLUTION TREATED + 464K (375°F) AGE:				
AGED 4 HRS/AC	36.0	23.0	51.0	39.5
AGED 8 HRS/AC	41.0	25.5	55.0	43.0
AGED 24 HRS/AC	38.5	24.0	55.0	42.0
AGED 72 HRS/AC	34.0	16.0	52.5	37.5

LOT NO.	COMPOSITION	EXTRUSION TEMPERATURE K	EXTRUSION TEMPERATURE (°F)	R_B HARDNESS AS EXTRUDED	R_B HARDNESS HEAT TREATED
1	Al-Fe-Co	700	(800)	72.0	73.5
2	Al-Fe-Co	755	(900)	67.5	69.5
5	Al-Li	755	(900)	40.0	41.0
5A	Al-Li	755	(900)	56.5	55.0
	EFFECT OF 25% HOT ROLLING AT 755 K (900°F)				
5	Al-Li	755	(900)	–	40.0
5A	Al-Li	755	(900)	–	50.5
	EFFECT OF INTERMEDIATE 25% COLD ROLLING				
5	Al-Li	755	(900)	39.5(A)	46.0(B)
5A	Al-Li	755	(900)	51.5(A)	53.5(B)

(A) AFTER SOLUTION TREATMENT + COLD ROLL
(B) AFTER FINAL AGING

Figure 6. – Thermomechanical treatment versus hardness of MA Al-Fe-Co and Al-Li alloys.

Based on the prior work[1], the solution heat treatment used for the Al-Fe-Co alloys was:

755K (900°F)/2 hours/Argon/AC.

Hardness values for these heat treated materials are shown in Figure 6.

Powder Metallurgy (PM)

The process sequence shown in Figure 7 was followed. Two 66 kg (145 lb) cold compacts of each alloy, 18.7 cm diameter (7.4 in.) by 109 cm long (42.9 in.), were formed in a wet bag system by isostatically pressing the powder at 207 MPa (30 ksi) to 75 percent of the alloy's theoretical density. The compacts were transferred into a 3003 aluminum cannister, sealed, and vacuum preheated for approximately one hour at 20-40 μm pressure. Differential scanning calorimetry was used to identify the solvus and solidus temperatures. The program schedule did not allow completion of the test before the scheduled hot pressing date. Consequently, the hot pressing temperature, 777K (940°F), was chosen from the Al-Cu-Mg phase diagram, Figure 3 (right, bottom), to avoid equilibrium melting at the ternary eutectic, 781K (946°F). The total heat-up cycle takes approximately seven to eight hours to complete. After the evacuation lines are sealed, the compacts were removed from the furnace and hot pressed at 621 MPa (90 ksi) to full density. The hot pressed PM billet is 71.7 cm (28.2 in.) long, from 21.4 cm diameter (8.4 in.) at the top to 23.4 cm (9.2 in.) at the bottom, to facilitate billet ejection from the hot pressing cylinder. The can material was removed by scalping the billet to 15.2 cm (6.0 in.) diameter and cutting 2.5 cm (1.0 in.) from each end. Additional 2.5 cm (1.0 in.) slices were cut off each end and saved for microstructural evaluation.

Extruding 2XXX Al alloys at 625K (666°F) necessitates shorter billet lengths to assure billet breakout. Breakout can occur at a higher temperature but at a 14 MPa (2 ksi) loss in strength[1]. Consequently, the billets were cut in half to approximately 30.5 cm (12 in.) long and extruded to the minimum 2.5 cm (1.0 in.) butt length to reduce material loss. Four billets from each alloy were extruded to 1.9 cm x 8.9 cm x 305 cm (0.75 in. x 3.5 in. x 120 in.) bars. The actual extrusion temperature, and the breakout and running pressures are listed in Figure 7 (lower right). Speed-displacement curves indicated that the front 61 cm (24 in.) of the extrusion did not experience steady state metal flow and was subsequently scrapped.

All extrusions were solution heat treated at 777K (940°F) instead of 766K (920°F) to assure that alloys PM 2618 and PM 2618 MOD B are fully resolution heat treated. Heating above the eutectic temperature, 781K (946°F), was avoided. After cold water quenching, the extrusions were stored in dry

ice to retard natural aging. Gauge marks were scribed on the bar to assure accurate stress relief stretch measurements. Figure 7 (upper right) shows a typical load-displacement curve from the stretcher indicating the propagation of Luders bands. Figure 7 (upper left) lists the temperature range, gauge length, and permanent set applied by stretching.

The effect of increasing the cold work on the tensile properties was discerned by an aging study. The aging response of the extrusions stretched 1.5 and 3.0 percent is assessed by heat treating the alloys at 436K (325°F) and 464K (375°F) for four aging times. The stretch-age conditions which produce the highest strength and best satisfies the minimum strength requirements for damage tolerance and high strength with corrosion resistance are selected in the initial property screen (see Table 3). The second property screen investigates the feasibility of increasing strength by a two step aging treatment. Incubation for 24 hours at 394K (250°F), 408K (275°F), and 422K (300°F) is followed by one, two, and four hour exposures at 464K (375°F).

Billet Microstructures. — The microstructure of the PM billet is illustrated by optical metallography in Figure 4. Guinier analysis of the phases present in the billets, Figure 3 (right, second box down) indicates that the phases detected are similar to those detected[10] in homogenized IM 2024 billets. The advantage obtained by PM processing is the fine size and distribution of the billet grains, and intermetallic particles which are normally present as large constituents in IM alloys. The fine distribution of Al_9FeNi and Al_7Cu_2Fe in PM 2618, and Al_7Cu_2Fe in PM HID 543 MOD and PM 2618 MOD B is shown in Figure 4 (second phases).

In IM 2618 which contains less Cu than PM 2618 and PM 2618 MOD B, equal Fe and Ni additions form only Al_9NiFe[3]. The presence of Al_7Cu_2Fe in alloy PM 2618 may be related to either the retention of Fe in supersaturated solid solution during solidification or the Cu addition shifting the alloy composition to a phase region where Al_7Cu_2Fe and Al_9NiFe co-exist. In alloy PM 2618 MOD B, the Fe present as an impurity forms Al_7Cu_2Fe. The phases $Al_6(Fe,Mn,Cr)$ and $Al_{20}Cu_2Mn_3$ were not detected in any of the alloys. Investigations[11] have shown that manganese co-exists in an intermediate $Al_7Cu_2(FeMn)$ phase. Only after sufficiently long annealing, an unidentified phase, presumably $Al_{20}Cu_2Mn_3$, precipitates[12].

Silicon is detected in all alloys in the form of Mg_2Si. The amount present is dependent on the quantity of Mg and Si available to form the stoichiometric compound. In alloy PM HID 543 MOD the amount formed is limited by the low Mg content, whereas in alloys PM 2618 and PM 2618 MOD B the amount formed is proportional to the Si level available.

STRETCH PARAMETERS OF THE EXTRUSIONS USED IN THE AGING STUDY AND PROPERTY EVALUATION												
ALLOY	① LENGTH (IN.)	① ELONG (IN.)	% ELONG	TEMP INIT K(F°)	TEMP FINAL K(F°)	ALLOY	① LENGTH (IN.)	① ELONG (IN.)	% ELONG	TEMP START K(F°)	TEMP FINISH K(F°)
PM HID 543 MOD	54	0.19 0.19	1.9 1.9	227 (–50)	249 (–10)	PM HID 543 MOD	107 5/8	3.02	6.04	274 (+35)	294 (+70)
PM HID 543 MOD	53 1/2	0.28 0.29	2.8 2.9	230 (–45)	247 (–14)	PM HID 543 MOD	107 5/8	3.15	6.30	269 (+25)	283 (+50)
						PM HID 543 MOD	107 7/8	3.10	6.20	266 (+20)	283 (+50)
PM 2618	53 3/4	0.32 0.32	3.2 3.2	230 (–45)	247 (–15)	PM 2618	107 3/4	2.98	5.98	255 (0)	275 (+36)
PM 2618	53 1/2	0.13 0.14	1.3 1.4	255 (0)	261 (+10)	PM 2618	108 3/16	3.11	6.22	247 (–15)	263 (+15)
						PM 2618	107 11/16	3.16	6.32	244 (–20)	263 (+15)
PM 2618 MOD B	54	0.19 0.19	1.9 1.9	233 (–40)	249 (–10)	PM 2618 MOD B	107 7/8	3.16	6.32	272 (+30)	280 (+45)
						PM 2618 MOD B	107 13/16	3.06	6.12	266 (+20)	280 (+45)
PM 2618 MOD B	53 7/8	0.29 0.28	2.9 2.8	238 (–30)	258 (+5)	PM 2618 MOD B	107 3/4	3.25	6.50	283 (+50)	294 (+70)

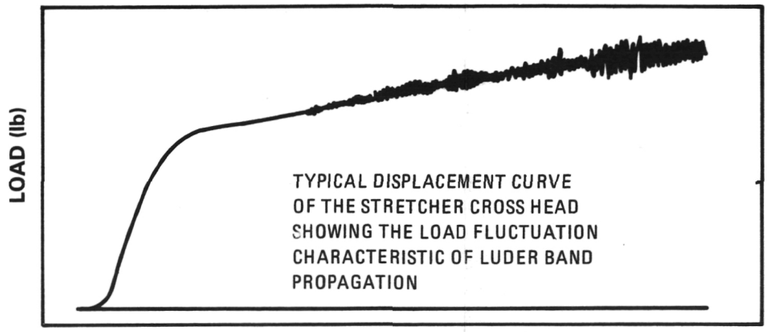

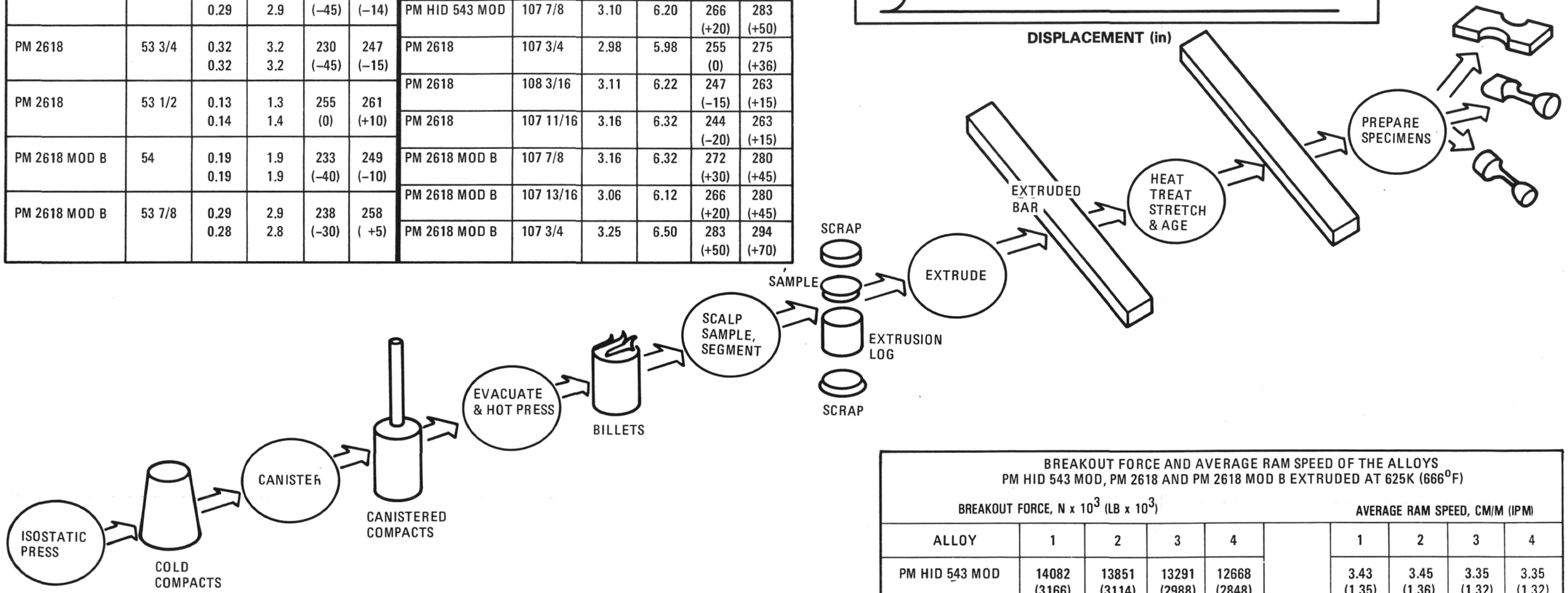

① CM = $\frac{IN}{2.54}$

BREAKOUT FORCE AND AVERAGE RAM SPEED OF THE ALLOYS PM HID 543 MOD, PM 2618 AND PM 2618 MOD B EXTRUDED AT 625K (666°F)									
	BREAKOUT FORCE, N x 10^3 (LB x 10^3)					AVERAGE RAM SPEED, CM/M (IPM)			
ALLOY	1	2	3	4		1	2	3	4
PM HID 543 MOD	14082 (3166)	13851 (3114)	13291 (2988)	12668 (2848)		3.43 (1.35)	3.45 (1.36)	3.35 (1.32)	3.35 (1.32)
PM 2618	16102 (3620)	15524 (3490)	16271 (3658)	16039 (3606)		3.35 (1.32)	3.53 (1.39)	3.40 (1.34)	3.48 (1.37)
PM 2618 MOD B	13798 (3102)	13486 (3032)	13460 (3026)	14190 (3190)		3.48 (1.37)	3.53 (1.39)	3.58 (1.41)	3.40 (1.34)

Figure 7. – PM process sequence with attendant extrusion and aging study stretch data.

Page Intentionally Left Blank

TABLE 3. – SMOOTH SPECIMEN TENSILE PROPERTIES FOR AGING TIMES AND TEMPERATURES AND VARYING DEGREES OF STRETCH (VALUES ARE AVERAGES OF DUPLICATE TESTS)

ALLOY	PM 2618				PM 2618 MOD B				PM HID 543 / MOD				PM 2618				PM 2618 MOD B				PM HID 543 MOD				PM 2618				PM 2618 MOD B				PM HID 543 MOD			
TEMP. K (2)	436				436				436				450				450				450				464				464				464			
STRETCH %		1.3	3.2	6.2		1.9	2.9	6.3		1.9	2.9	6.2		1.3	3.2	6.2		1.9	2.9	6.3		1.9	2.8	6.2		1.3	3.2	6.2		1.8	2.9	6.0		1.9	2.8	6.2
YIELD STRENGTH MPa (1)	0 HR	359.5	382.0	412.0	0 HR	387.5	405.0	433.0	0 HR	338.5	357.0	405.0	0 HR	359.5	382.0	412.0	0 HR			433.0	0 HR			405.0	0 HR	359.5	382.0	412.0	0 HR			433.0	0 HR			405.0
	4	352.8	373.3	428.0	4	374.8	388.3	437.0	4	329.3	344.5	413.0	2	339.8	380.8	410.0	2	369.8	389.5	435.0	2	327.5	336.8	407.0	2	336.0	385.0	436.0	2	397.8	412.0	463.0	2	322.5	349.8	425.2
	8	347.0	366.0	425.0	8	384.8	399.3	447.0	8	353.3	375.5	432.0	4	336.8	374.0	425.0	4	388.5	396.0	449.0	4	346.5	367.0	434.0	4	349.8	402.8	449.0	4	417.5	424.3	473.0	4	335.5	357.3	418.0
	16	343.8	382.0	446.0	16	397.3	412.0	476.0	16	371.8	384.8	440.0	8	341.8	386.3	446.0	8	392.5	412.5	467.0	8	356.8	372.3	422.0	8	363.5	402.0	426.0	8	404.3	410.3	440.0	8	333.3	343.3	385.0
	32	345.8	391.0	449.0	32	406.3	424.5	479.0	32	370.8	378.5	412.0	16	368.0	414.5	454.0	16	421.3	427.8	478.0	16	346.3	372.5	418.0	12	357.8	391.3	414.0	12	388.0	393.8	431.0	12	321.3	341.3	398.5
ULTIMATE TENSILE STRENGTH MPa (1)	0	469.5	477.5	464.5	0	506.0	513.5	499.5	0	460.0	455.5	461.5	0				0				0				0				0				0			
	4	461.3	468.5	495.2	4	485.8	488.0	511.2	4	461.0	458.5	493.8	2	454.5	470.0	483.5	2	481.0	487.3	504.2	2	445.8	437.3	480.2	2	438.5	451.8	479.2	2	480.3	478.0	475.2	2	408.8	420.5	481.2
	8	458.3	447.5	490.5	8	487.3	490.3	510.5	8	466.3	466.5	496.8	4	450.3	459.5	482.2	4	483.0	482.8	501.2	4	442.0	449.0	488.2	4	424.5	446.3	474.8	4	471.0	472.0	498.8	4	412.5	427.0	473.2
	16	452.3	466.8	495.5	16	488.8	490.0	517.0	16	461.5	460.3	488.0	8	440.0	455.0	482.0	8	473.3	474.8	501.0	8	438.0	441.3	473.0	8	419.5	440.3	456.5	8	451.0	455.0	475.2	8	410.8	418.3	442.0
	32	444.5	459.0	480.2	32	478.8	485.0	504.5	32	449.0	447.3	475.2	16	450.8	454.4	476.0	16	467.5	470.5	500.8	16	422.0	426.3	473.0	12	412.5	435.0	451.8	12	440.3	446.0	469.0	12	402.5	416.5	460.2
REDUCTION AREA %	0	16.0	22.0	18.5	0	16.0	18.0	15.5	0	10.0	23.0	23.0	0				0				0				0				0				0			
	4	18.5	20.0	17.0	4	18.5	18.5	18.5	4	24.5	26.5	29.0	2	17.0	18.5	23.0	2	21.0	19.0	19.5	2	23.5	23.5	26.5	2	19.0	24.0	31.5	2	22.5	22.0	29.0	2	30.5	33.5	31.0
	8	18.5	26.0	24.0	8	22.0	19.5	19.0	8	29.5	27.0	30.5	4	21.0	18.0	28.5	4	21.5	26.0	20.0	4	29.0	32.5	30.0	4	31.0	36.5	40.0	4	28.0	29.0	31.0	4	41.5	40.0	43.0
	16	26.5	22.5	20.5	16	24.0	24.0	26.5	16	27.0	33.0	34.5	8	23.0	28.5	31.0	8	26.5	23.0	26.0	8	34.0	34.0	37.0	8	41.5	46.0	48.5	8	31.5	36.0	29.5	8	42.0	42.0	42.0
	32	25.0	29.5	30.5	32	24.5	25.5	27.5	32	34.5	29.0	40.0	16	26.5	33.0	38.0	16	32.5	22.0	32.5	16	42.0	36.5	42.5	12	44.5	48.0	45.5	12	33.0	35.0	35.0	12	42.5	38.5	43.0
ELONGATION %	0	13.2	16.1	10.2	0	15.2	16.1	12.2	0	14.2	17.1	11.2	0				0				0				0				0				0			
	4	15.6	16.1	13.2	4	16.6	15.6	14.2	4	20.6	18.6	16.2	2	13.7	16.1	14.2	2	15.6	15.6	15.7	2	19.1	17.6	16.2	2	12.0	16.6	9.8	2	14.2	15.1	12.7	2	15.2	13.7	13.2
	8	15.6	15.6	13.2	8	17.6	17.6	14.7	8	18.6	16.1	14.2	4	14.2	16.1	9.8	4	16.6	16.6	13.7	4	16.1	15.6	12.7	4	14.2	15.2	11.7	4	12.7	12.2	11.2	4	14.7	15.1	15.2
	16	15.1	15.2	11.7	16	16.6	16.1	13.2	16	15.2	15.6	13.2	8	14.6	14.6	13.2	8	15.2	13.7	11.7	8	14.7	14.2	14.2	8	13.0	13.7	14.2	8	13.2	12.7	11.7	8	15.2	15.2	14.2
	32	14.6	14.6	11.2	32	13.2	14.2	11.7	32	15.1	13.2	13.2	16	14.2	14.7	12.2	16	12.7	11.2	11.2	16	14.7	14.2	13.2	12	13.2	15.2	13.7	12	12.7	13.2	12.2	12	15.2	14.7	14.7

(1) $\frac{\text{MPa}}{6.895}$ = KSI

(2) TK x 1.8 – 459 = $T^{o}F$

Page Intentionally Left Blank

The amount of primary soluble phases, Al_2Cu and Al_2CuMg, indicates that the segregation created during solidification is not eliminated by the precipitation and growth of the phase present in the atomized powder, Figure 3 (upper left). The one hour hold at 777K (940°F) during the vacuum pre-heating cycle appears inadequate to dissolve the large equilibrium Al_2Cu which forms.

Extrusion Microstructures.- Longitudinal metallographic sections of the extrusions are illustrated in Figure 4. Figure 4 also reveals that the grain structure at the front of the extrusion is coarser than at the rear. The grain structure at the interior (T/2) is coarser than near the surface (T/10). A recrystallized layer is observed on the surface of alloys PM HID 543 MOd and PM 2618 MOD B. The thickness of the recrystallized layer is greatest at the rear. The presence of the dispersoid sized constituents in PM 2618 eliminates the large recrystallized grains on the surface of the bar and promotes an overall finer grain structure.

The variation in grain structure appears related to the different strain histories experienced through the thickness and along the length of the extruded bar. A finer grain structure is associated with the more severely strained locations closer to the surface[5] and at the rear of the extrusion. Pinhole X-ray patterns in Figure 8 indicate that the finer structure is less recrystallized. Although a significant difference in grain structure is observed between PM 2618 and PM 2618 MOD B, Figure 4, discerning differences in the degree of recrystallization with pinhole patterns as shown in Figure 8 was not possible.

Thermomechanical Study.- For these precipitation hardening materials, strengthening depends on a combination of high subgranular dislocation density (work induced) and very fine, strong, and closely spaced precipitates and dispersoids (composition and time-temperature dependent). The procedure for solution treatment time at temperature, quench rate, and particularly the degree of post heat treat stretch along with artificial aging time at temperature must be explored and optimized. Peak tensile yield strengths attainable from variations in stretch and single step aging times at temperatures were measured, recorded (Table 3), and plotted (Figure 9). The results indicate that the strength of the alloys with 1.5 and 3.0 percent stretch falls short of the design minimum target values for damage tolerance; assuming that minimum values for heat treatable alloys are approximately 34.5 MPa (5 ksi) less than the observed typical values. Consequently, the alloys were stretched 6.0 percent (double conventional mill practice) in an attempt to achieve the target values. Although the strengths of PM HID 543 MOD and PM 2618 in the 6.0 percent stretch condition are close to the program target values, only PM 2618 MOD B meets the program target value. Figure 10 was used to select the optimum aging conditions for the θ and S precipitating alloys stretched to 6.0 percent: 16 hours

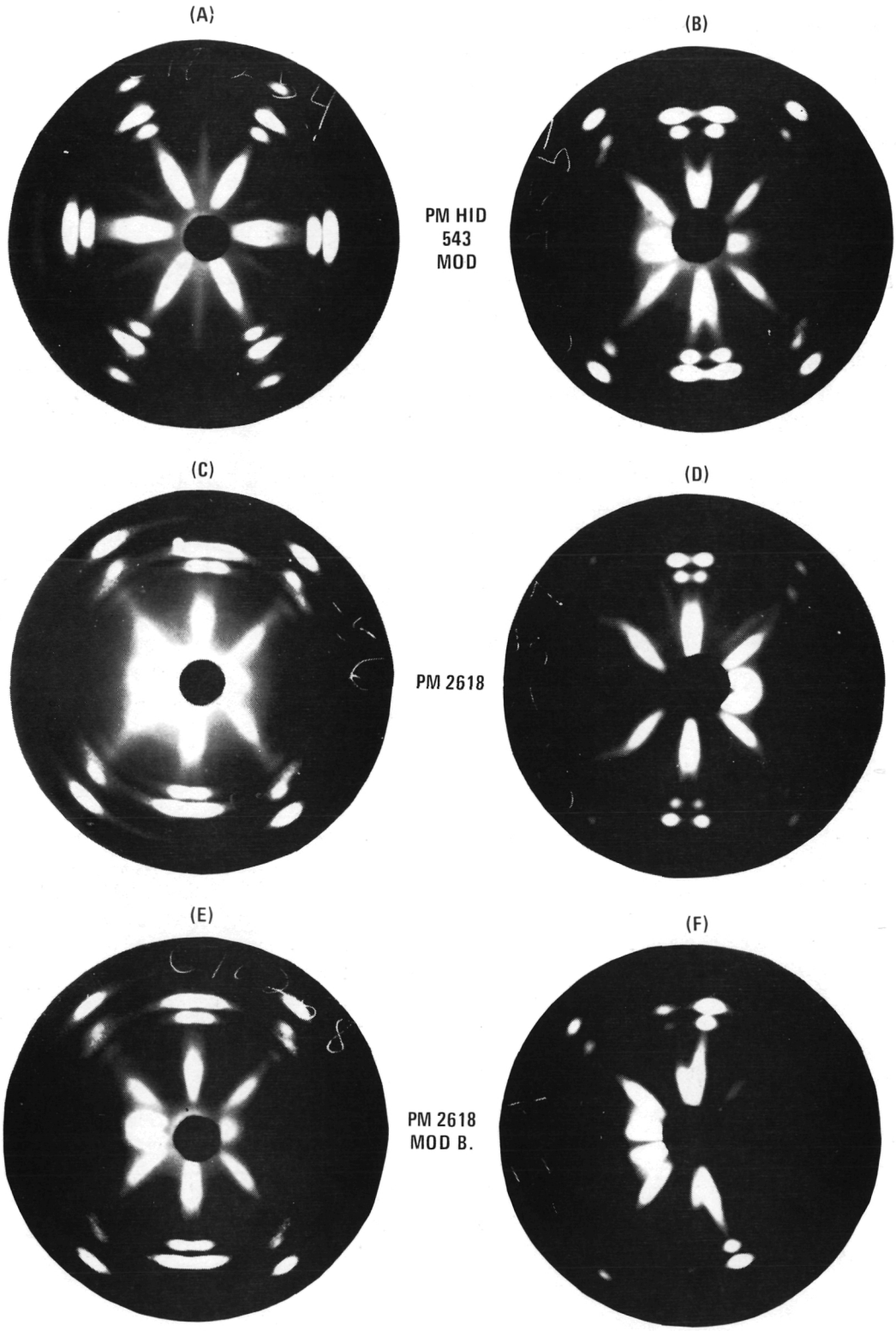

Figure 8. – Pinhole x-ray patterns indicating that the front of the extrusion is more recrystallized than the rear.

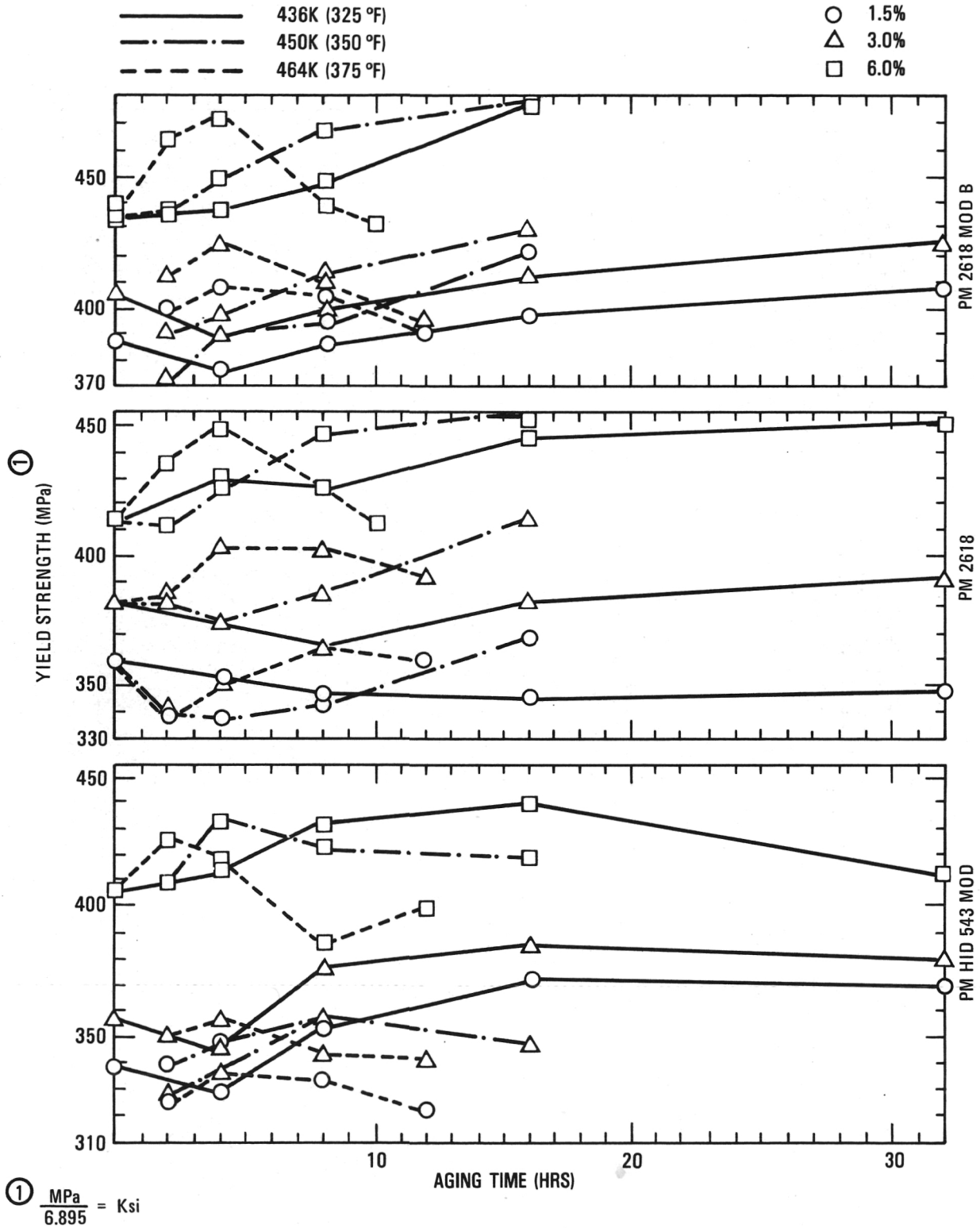

Figure 9. – Aging response showing the effect of aging temperature and strength.

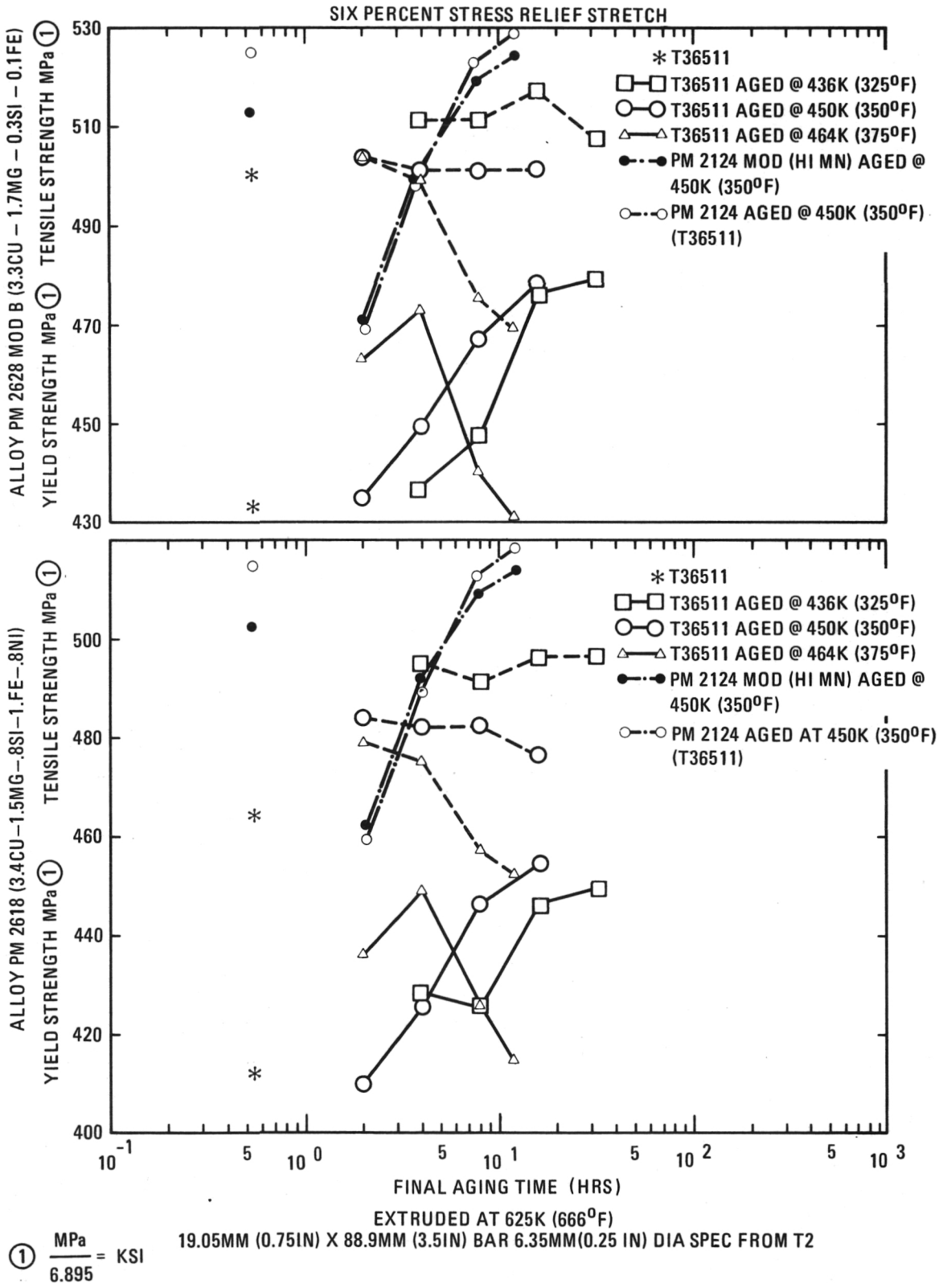

Figure 10. – Aging curves showing the similar aging response of PM 2XXX alloys with a 2.2:1 Cu/Mg ratio at different solute contents.

at 436K (325°F) and 450K (350°F), respectively, for PM HID 543 MOD, and for PM 2618 and PM 2618 MOD B. Table 4 lists the strength improvements at 1.9 cm (0.75 in.) thickness and 3 percent stretch achieved by PM processing. The results indicate that significant improvements in yield strength can be achieved, especially in the natural aged condition.

The aging response of the alloys depends on the stretch magnitude and the aging temperature. Figure 11 shows that the yield strength is particularly sensitive to the stretch. Figure 9 reveals that increasing the amount of cold work accelerates the aging response for θ and S precipitating alloys. The maximum obtainable strength decreases with increasing aging temperature in the Al-Cu alloy, PM HID 543. In the Al-Cu-Mg alloys, PM 2618 and PM 2618 MOD B, the peak yield strength is less sensitive to the aging temperatures investigated.

The aging response of the five percent cold rolled and stretched PM 2124 peak artificially aged alloys in the previous study is similar to that of the present alloys except for the initial softening after two hours exposure at 450K (350°F), Figure 10. Conversely, the aging response of 1.63 mm (0.064 in.) IM 2618 sheet[13] is two to four times as sluggish at 450K (350°F) and 464K (375°F), respectively. Strengthening 2XXX Al alloys in the naturally aged (NA) and artificially aged (AA) temper is accomplished by increasing the degree of cold work applied after solution heat treatment. In the NA temper, the strengthening is due to the cold work increasing the dislocation density since the G.P. zone size and distribution does not vary at room temperature. The improvement in the NA yield strength of PM alloys over their IM counterparts may be related to a higher dislocation density. During deformation, a material need only deform by multiple slip adjacent to the grain boundary[14]. The smaller grain size of the PM extrusion may therefore increase the dislocation density during stretching relative to the larger grain IM counterpart. Additionally, the smaller grain size may slightly improve the strength by reducing the distance between major deformation barriers.

The propensity of θ" and S" to nucleate on dislocations allows cold work to be an effective method for improving the strength of 2XXX alloys. Except for lower aging times in the underaged condition, increasing the dislocation density strengthens the alloy not only by decreasing the size and distribution of the intermediate precipitate, but decreases the precipitate size range[15]. Investigations[15] have shown that increasing the dislocation density by cold work accelerates the aging response either by increasing the kinetics of the precipitation sequence or by generating a greater number of intermediate precipitates which nucleate at the onset of aging. The accelerated aging response of the PM alloy PM 2618 relative to IM 2618 sheet is probably due to the lower degree of recrystallization, hence, a higher dislocation density. The two step aging data presented in Table 5 indicates no improvement in strength for the combination of time and temperature investigated. The approach was subsequently abandoned. Apparently, heterogeneous nucleation of S' on dislocations provides a finer distribution than obtained by homogeneous nucleation at the temperatures investigated. The

TABLE 4. – YIELD STRENGTH IMPROVEMENT ACHIEVED BY PM 2124 AND HIGH CU 2618 OVER CONVENTIONAL IM 2XXX ALLOYS

ALLOY	TEMPER	THICKNESS OR PRODUCT SIZE		THESE DATA OBTAINED FROM PREVIOUS YEAR (SEE REF. 1)						PM 2618			PM 2618 MOD B (No Fe, Ni)		
				PM 2124 Hi MN			PM 2124								
		(IN)	(CM)	KSI	MPa	%	KSI	MPa	%	KSI	MPa	%	KSI	MPa	%
2224	T3511*	0.75 x 1.5	1.9 x 3.8	5.8	40.0	10.5	5.8	40.0	10.5	0.4	2.8	0.7	3.7	25.5	4.7
2224	T8511	0.80 x 2.8	20 x 7.1	8.1	55.9	14.1	8.5	58.6	14.7	2.4	16.6	4.2	4.4	30.4	7.6
2024	T8511*	≥1.5	≥3.8	3.8	20.2	6.6	3.8	26.2	6.6	-1.6	-11.0	-2.8	-1.7	-11.7	-3.0
2024	T8511*	≥0.25	≥0.64	2.7	18.6	4.3	3.1	21.4	4.9	-3.0	-20.4	-4.8	-1.0	-6.9	-1.6
2124	T351	1.0 – 2.0	2.5 – 5.1	10	69.0	19.4	10	69.0	19.4	4.6	31.7	8.8	7.9	54.5	15.3
2124	T851	1.5 – 2.0	3.8 – 5.1	0.0	0.0	0.0	0.4	2.8	0.6	-5.7	-39.3	-8.7	-3.7	-25.5	-5.6
2324	T39+	1.25 – 1.5	3.2 – 3.8	9.2	63.5	13.3	6.7	46.2	10.0	-7.1	-11.0	-10.6	-4.2	-28.9	-6.2
X2034	T351	0.5	1.27	5.8	40.0	10.5	5.8	40.0	10.5	0.4	2.8	0.7	3.7	– 25.5	6.7

*F_{ty}+34.5 MPa (5 KSI)

+2324-T39 IS COLD ROLLED 9 – 13% AND IS COMPARED TO THE PM ALLOYS IN THE T36511 TEMPER, I.E., COLD ROLLED 5% AND STRETCHED 1.5% OR STRETCHED 6.0%

(1) IM DATA USED IN THIS COMPARISON WAS GENERATED IN THE COURSE OF AN ALCOA INDEPENDENT RESEARCH AND DEVELOPMENT PROGRAM

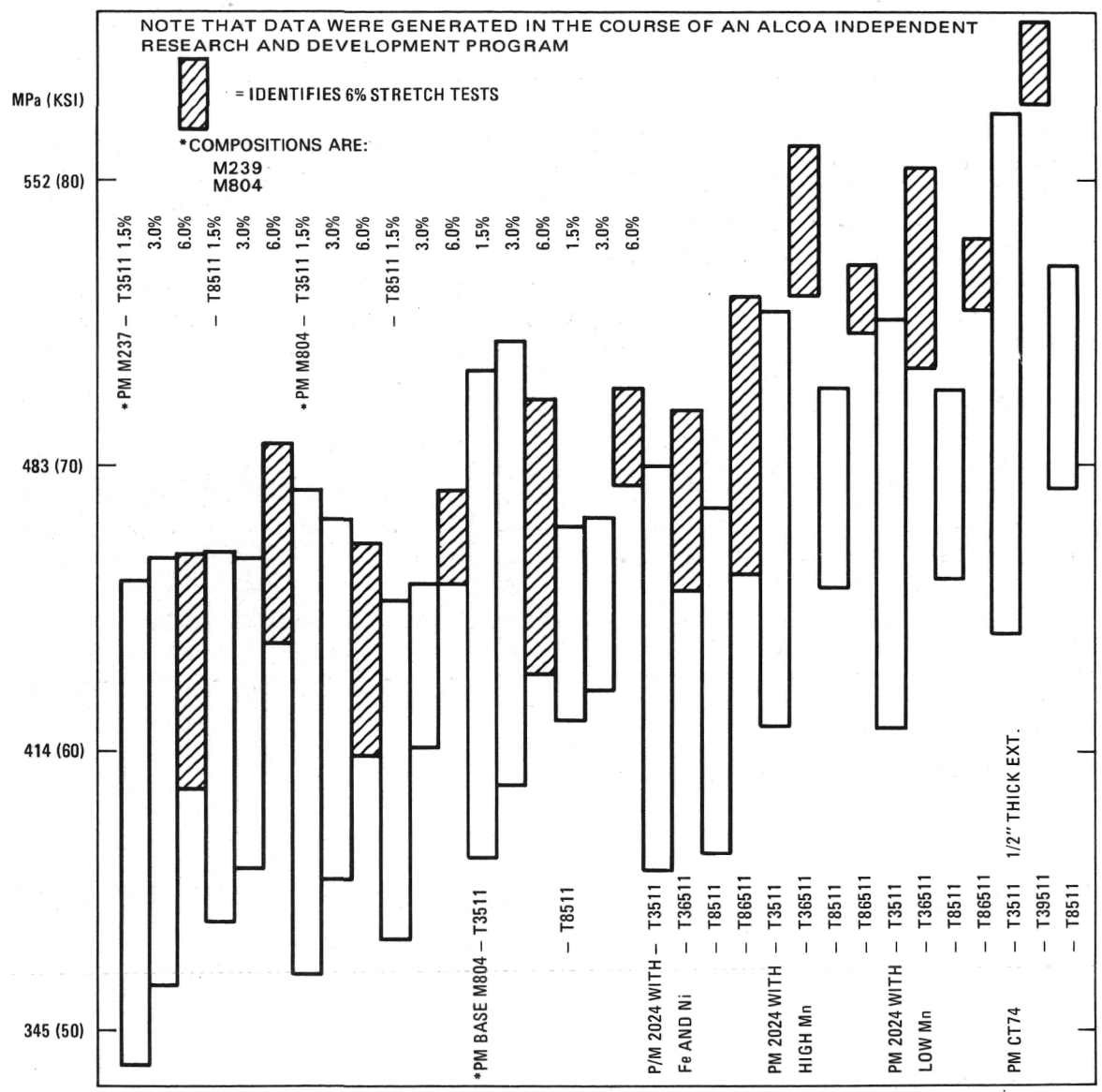

Figure 11. – Typical yield and tensile strengths of PM 2XXX extrusions.

TABLE 5. – TENSILE PROPERTIES FROM THE 2-STEP AGING STUDY USING 3 INCUBATION TEMPERATURES AND ONE FINAL AGING TEMPERATURE AT 464K (375°F)

PROPERTIES	HRS FINAL AGE 464 K ②	PM HID 543 MOD TEMP. K ②			PM 2618 TEMP. K ②			PM 2618 MOD B TEMP. K ②		
		322	329	339	322	329	339	322	329	339
STRETCH YIELD STRENGTH MPa①	0	433.0	433.0	433.0						
	1	412.8	410.5	415.0	418.0	402.0	429.8	428.5	456.0	439.0
	2	415.0	414.0	418.0	439.5	419.5	421.5	458.5	451.0	452.5
	4	412.5	419.5	418.5	452.0	444.0	453.8	475.0	499.0	468.0
ULTIMATE TENSILE STRENGTH MPa①	0	499.5	499.5	499.5						
	1	479.0	471.0	474.0	482.0	480.2	477.2	494.0	512.0	500.0
	2	463.0	462.0	472.0	479.0	466.5	468.0	496.0	493.5	493.0
	4	465.5	467.0	472.0	477.0	472.5	478.0	502.0	498.8	495.0
REDUCTION AREA %	0	15.5	15.5	15.5						
	1	26.0	27.0	25.0	25.0	22.5	25.5	24.5	24.0	23.0
	2	34.0	32.0	33.5	30.5	32.5	26.0	24.0	27.5	23.0
	4	39.5	38.5	37.5	37.5	39.0	36.0	27.5	32.0	32.5
ELONGATION %	0	12.2	12.2	12.2						
	1	13.2	14.2	12.7	13.2	13.2	12.2	16.0	14.2	15.2
	2	13.2	13.2	13.2	12.7	13.7	13.2	12.2	13.2	12.2
	4	14.2	13.2	12.7	12.7	13.2	12.7	11.2	11.2	11.2

① $\frac{MPa}{6.895}$ = KSI ② TK x 1.8 - 459 = T°F

similar behavior of the final aging step at 464K (375°F) to the single step aging treatment at 464K (375°F), Figure 12, indicates that the GP zone solvus is at a higher temperature. However, aging at higher temperatures will probably result in a further reduction in strength. Slower heating rates may prove successful.

Examination of the results in Figure 9 shows that the Fe and Ni additions to alloy 2618 MOD B reduce the yield strength approximately five percent. In the previous survey[1], Fe and Ni additions in lieu of Mn to a 2124 base composition reduced the yield strength of alloy PM 2618 MOD A (high Si, Fe, low Ni) at least 16 percent. Equal Fe and Ni additions in IM 2618 do not affect strength[3]. The addition of either Fe or Ni reduces strength by forming Cu-rich, Fe or Ni phases. However, equal additions of Fe and Ni to a high Cu 2618 base, PM 2618 MOD B, reduces strength. Guinier X-ray analysis of PM 2618 reveals that some of the Fe forms Al_7Cu_2Fe in lieu of

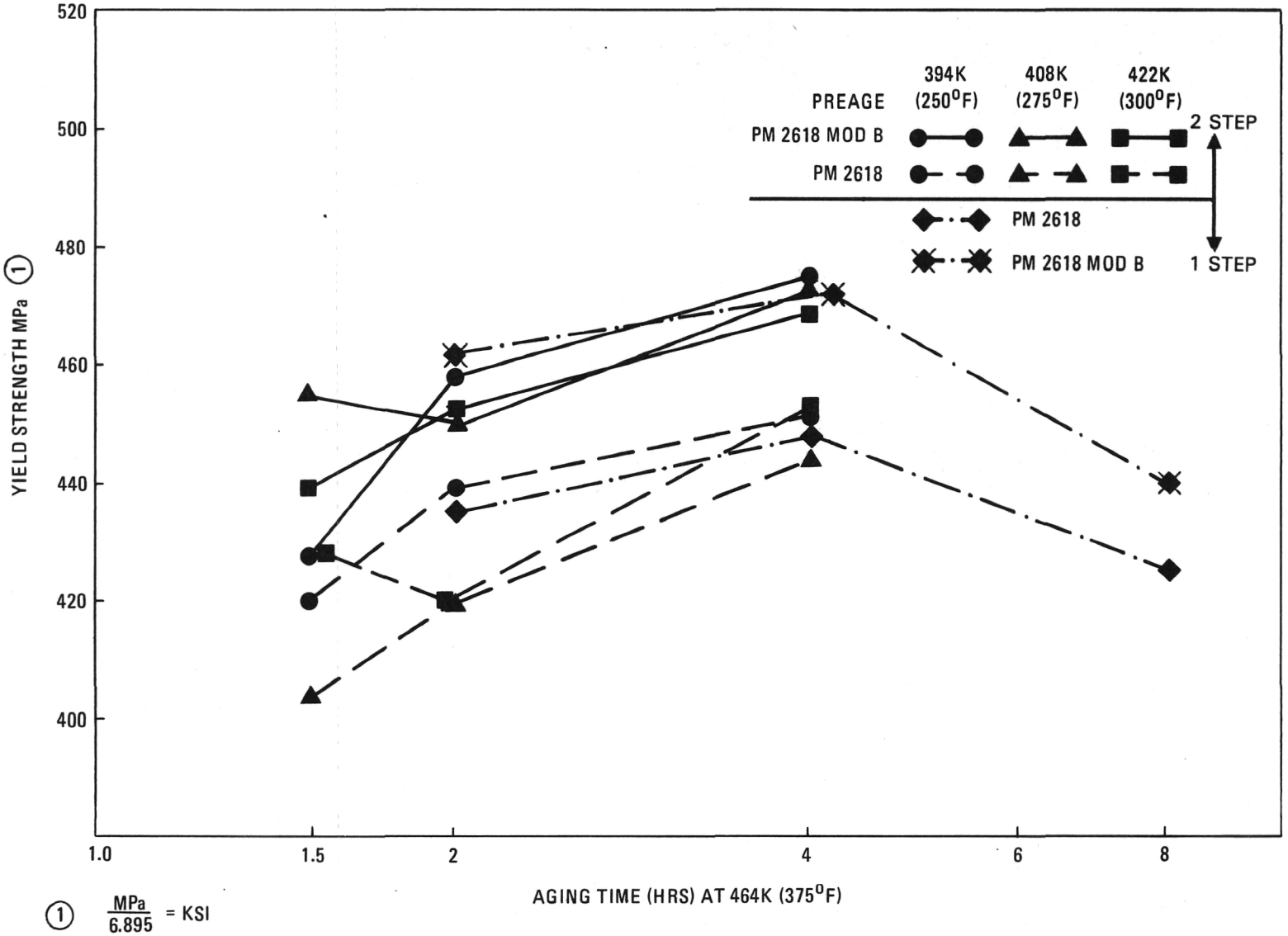

Figure 12. – The similar aging response of two step to single step aging treatments.

Al_9FeNi as suggested by the 1:1 Fe/Ni ratio. Figure 3 (upper right) lists the calculated weight percent of Cu available after the precipitation of insoluble Cu and Mg phases during hot pressing[16]. The bulk and actual compositions of the PM high Cu 2618 and 2124 alloys are plotted on the Al-Cu-Mg solvus diagram, Figure 3 (lower left). The results show that lower strength of the Fe and Ni containing alloys, PM 2618 MOD A and PM 2618, is probably due in part to a lower Cu content. Greater strength is observed for the higher Cu containing PM 2124 alloys[1]. However, the strength of the 0.5 wt. pct. Mn PM 2124 alloy is only 6.9 - 13.8 MPa (1-2 ksi) greater than the 1.5 wt. pct. Mn PM 2124 alloy which contains approximately 1.0 wt. pct. less Cu. The alloys display similar strength as a consequence of the solution heat treatment used. At 766K (920°F), only slightly more Cu in PM 2124 is put in solid solution than PM 2124 MOD (high Mn), hence, a similar volume fraction of strengthening phase precipitates. Similarly, the strength of PM 2618 MOD A and PM 2124 MOD (high Mn) is nearly identical. Therefore, strength in 2XXX Al alloys with similar texture and grain size is strongly dependent on secondary alloy additions which consume Cu and are dependent on the maximum usable solution heat treatment temperature.

Preliminary X-ray data and metallography indicate most of the soluble Cu and Mg phases in alloy PM 2618 and alloy PM 2618 MOD B are in solution after two hours exposure at 777K (940°F). In the alloy PM HID 543 MOD, much of the equilibrium Al_2Cu phase is retained after two hour exposure at 777K (940°F). Increasing the solution heat treatment temperature to 788K (960°F) and 800K (980°F) progressively dissolves more of the soluble phase. Higher solution heat treatment temperatures than used for hot pressing, such as 802K (985°F) used for IM 2219, should improve the strength of PM HID 543 MOD by increasing the supersaturation. The potential for improving the strength of alloy PM HID 543 MOD above program goals is favorable.

Test Details

Mechanically Alloyed Powder Metallurgy (MAPM)

The tensile properties of the four extruded alloys were obtained in the heat treated condition at room temperature, and elevated temperatures of 394K (250°F) and 450K (350°F). Room temperature and elevated temperature tensile tests were also conducted after 1000 hour exposure at 394K (250°F) and 450K (350°F) to determine the structural stability of the MA alloys. Tests were conducted at room temperature according to ASTM Standard E-8, and at elevated temperature according to ASTM Standard E-21 on Tinius Olsen Universal Testers using a 6.4 mm (0.25 in.) tensile specimen (Figure 5). Notched tensile properties at room temperature were also determined as a preliminary indication of the fracture toughness levels for these MA alloys using the notched tensile specimen shown in Figure 5.

Powder Metallurgy (PM)

All 6.4 mm (0.25 in.) diameter smooth and 12.7 mm (0.50 in.) diameter notched tensile specimens were machined to ASTM specifications from longitudinal blanks cut at least 1.27 cm (0.5 in.) from the edge of the bar to avoid differences in the type of texture. All values reported are an average of duplicate tests. Notched tensile tests are used as a fracture toughness indicator to aid in the selection of the aging treatment with the optimum combination of strength and notched tensile strength for each alloy.

RESULTS AND DISCUSSION

Mechanically Alloyed Powder Metallurgy (MAPM)

Structural evaluation, after heat treatment, was performed using optical metallography. Standard specimen preparation techniques were used. Heat treated structures were recorded at 200X and 1000X in the longitudinal plane. The Al-Fe-Co specimens were etched in 10 percent NaOH, while a 20 percent H_3PO_4 etch was used for the Al-Li specimens. The structures for these alloys are shown in Figures 1 and 2. The Al-Fe-Co alloys (Figure 1) generally show a uniform dispersion of an equiaxed secondary phase. Although some stringers of light etching areas were occasionally noted, these structures are markedly cleaner in appearance than those previously produced[1], even though the current materials are substantially higher in alloy content. The Al-Li alloys (Figure 2) show a uniform distribution of precipitates and dispersoids, which increases as the dispersoid content increases. Also evident is a heavier precipitation at areas which may be related to prior particle boundaries.

Tensile Tests at 294K (70°F)

Table 6 lists the smooth bar tensile properties for the alloys produced. The MA Al-Fe-Co alloys show an increase in strength with a decrease in extrusion temperature. An increased dispersoid content in the MA Al-Li alloy (Lot 5A) also results in increased strength and a loss in ductility. As was expected, the mild hot working given the MA Al-Li alloys resulted in slight strength reductions, coupled with a small improvement in ductility. In a similar manner, the intermediate cold rolling applied to the MA Al-Li alloys resulted in strength improvements and ductility losses. The strength levels of the MA Al-Li alloys are well below those values previously obtained[1], but show a significant improvement in ductility.

Notched Tensile Tests at 294K (70°F)

The notched tensile properties for the four alloys are shown in Table 6. Evaluation of notched tensile properties and determination of notched ratios

TABLE 6. – TENSILE PROPERTIES (SMOOTH AND NOTCHED) AT AMBIENT AND ELEVATED TEMPERATURES FOR MA ALLOYS

TEMPERATURE				NOMINAL COMPOSITION	LOT NO.	UNMEASURED DURATION AT 297K (70°F)						1000-HOUR EXPOSURE AT 394K (250°F)						1000-HOUR EXPOSURE AT 450K (350°F)					
TENSION TEST		EXTRUSION				YIELD STRENGTH		UTS		El. %	RA %	YIELD STRENGTH		UTS		El. %	RA %	YIELD STRENGTH		UTS		El. %	RA %
K	(°F)	K	(°F)			MPa	(KSI)	MPa	(KSI)			MPa	(KSI)	MPa	(KSI)			MPa	(KSI)	MPa	(KSI)		
297	(70)	700	(800)	Al-Fe-Co	1	359.9	(52.2)	416.4	(60.4)	5.0	9.3	388.9	(56.4)	431.6	(62.6)	4.0	8.0	386.1	(56.0)	432.3	(62.7)	3.0	6.8
		755	(900)	Al-Fe-Co	2	332.3	(48.2)	391.6	(56.8)	4.0	7.8	347.5	(50.4)	402.7	(58.4)	5.5	8.5	344.0	(49.9)	400.6	(58.1)	4.5	7.8
		755	(900)	Al-Li	5	236.5	(34.3)	283.4	(41.1)	15.5	35.5	255.8	(37.1)	301.3	(43.7)	12.5	30.0	233.7	(33.9)	277.9	(40.3)	14.0	26.0
		755	(900)	Al-Li	5A	278.5	(40.4)	324.1	(47.0)	12.0	25.8	284.1	(41.2)	330.9	(48.0)	11.0	20.0	273.0	(39.6)	317.2	(46.0)	11.0	13.0
						EFFECT OF 25% HOT ROLLING AT 755K (900°F)																	
		755	(900)	Al-Li	5	225.4	(32.7)	277.2	(40.2)	16.5	39.3												
		755	(900)	Al-Li	5A	259.9	(37.7)	312.3	(45.3)	12.5	27.8												
						EFFECT OF INTERMEDIATE 25% COLD ROLLING																	
		755	(900)	Al-Li	5	262.7	(38.1)	315.1	(45.7)	10.5	27.8												
		755	(900)	Al-Li	5A	281.3	(40.8)	348.2	(50.5)	9.5	20.5												
394	(250)	700	(800)	Al-Fe-Co	1	325.4	(47.2)	362.0	(52.5)	4.0	9.5	320.6	(46.5)	357.8	(51.9)	3.0	6.0	288.2	(41.8)	328.2	(47.6)	3.0	4.0
		755	(900)	Al-Fe-Co	2	289.6	(42.0)	331.6	(48.1)	4.0	5.5	289.6	(42.0)	332.3	(48.2)	3.5	5.3	253.7	(36.8)	295.8	(42.9)	3.5	5.0
		755	(900)	Al-Li	5	182.0	(26.4)	206.2	(29.9)	24.5	51.5	195.1	(28.3)	229.6	(33.3)	21.5	44.0	122.0	(17.7)	158.6	(23.0)	34.0	41.5
		755	(900)	Al-Li	5A	213.7	(31.0)	253.7	(36.8)	18.5	38.8	215.1	(31.2)	257.2	(37.3)	18.5	33.8	129.6	(18.8)	180.0	(28.1)	24.0	31.8
						EFFECT OF 25% HOT ROLLING AT 755K (900°F)																	
		755	(900)	Al-Li	5	179.6	(26.1)	208.2	(30.2)	24.5	51.5												
		755	(900)	Al-Li	5A	202.0	(29.3)	236.5	(34.3)	20.5	39.5												
						EFFECT OF INTERMEDIATE 25% COLD ROLLING																	
		755	(900)	Al-Li	5	202.7	(29.4)	242.0	(35.1)	28.5	42.0												
		755	(900)	Al-Li	5A	208.2	(30.2)	260.6	(37.8)	11.5	24.3												
450	(350)	700	(800)	Al-Fe-Co	1	281.3	(40.8)	322.7	(46.8)	5.0	10.3												
		755	(900)	Al-Fe-Co	2	259.9	(37.7)	299.2	(43.4)	4.0	6.3												
		755	(900)	Al-Li	5	110.3	(16.0)	157.9	(22.9)	35.5	43.8												
		755	(900)	Al-Li	5A	148.2	(21.5)	195.8	(28.4)	27.5	39.5												
						EFFECT OF 25% HOT ROLLING AT 755K (900°F)																	
		755	(900)	Al-Li	5	107.6	(15.6)	153.1	(22.2)	30.5	37.0												
		755	(900)	Al-Li	5A	126.2	(18.3)	173.4	(25.2)	34.5	42.5												
						EFFECT OF 25% INTERMEDIATE COLD ROLLING																	
		755	(900)	Al-Li	5	124.8	(18.1)	175.8	(25.5)	23.5	38.5												
		755	(900)	Al-Li	5A	129.6	(18.8)	193.7	(28.1)	16.5	24.5												

NOTCHED TENSILE PROPERTIES AT 297K (70°F)

LOT NO.	COMPOSITION	EXTRUSION TEMPERATURE K	(°F)	NOTCHED TENSILE STRENGTH MPa	(KSI)	NOTCH RATIOS YIELD	UTS
1	Al-Fe-Co	700	(800)	397.1	(57.6)	1.10	0.95
2	Al-Fe-Co	755	(900)	383.4	(55.6)	1.15	0.98
5	Al-Li	755	(900)	404.7	(58.7)	1.71	1.43
5A	Al-Li	755	(900)	457.1	(66.3)	1.64	1.41
	EFFECT OF 25% HOT ROLLING AT 755K (900°F)						
5	Al-Li	755	(900)	382.0	(55.4)	1.70	1.38
5A	Al-Li	755	(900)	439.2	(63.7)	1.69	1.41
	EFFECT OF INTERMEDIATE 25% COLD ROLLING						
5	Al-Li	755	(900)	440.6	(63.9)	1.68	1.40
5A	Al-Li	755	(900)	488.1	(70.8)	1.74	1.40

were used as a preliminary indication of alloy toughness. The notched ratios for the MA Al-Fe-Co alloys improve slightly as extrusion temperature increases and follows the same trend as previously observed in the MA Al-Fe-Co alloys[1]. The current values are similar to those previously obtained for a 644K (700°F) extrusion temperature and may be a reflection of the higher alloy content used in the present study. The MA Al-Li alloys exhibit an excellent notched toughness. Neither hot nor cold working had any significant effect on notched properties.

Tensile Tests at 394K (250°F) and 450K (350°F)

Smooth bar tensile properties at 394K (250°F) and 450K (350°F) are listed in Table 6. At 394K (250°F) the MA Al-Fe-Co alloys retain 85 percent of their room temperature strength with no appreciable loss in ductility. At this same temperature, the MA Al-Li alloys retained 75 percent of their room temperature strength and exhibited significant improvements in ductility.

As the test temperature is increased to 450K (350°F), the MA Al-Fe-Co alloys still retain 75 percent of their room temperature levels with no appreciable change in ductility. An approximate strength loss of 50 percent was obtained in the MA Al-Li alloys at this temperature, coupled with approximately a 100 percent increase in ductility.

Tensile Tests after 1000 Hour Exposure at 394K (250°F) and 450K (350°F)

Room temperature tensile properties for smooth bars, after having been exposed for 1000 hours at either 394K (250°F) or 450K (350°F), are shown in Table 6. All four alloys exhibit a slight improvement in strength after the long time exposure at 394K (250°F) with only a slight effect on ductility. After 1000 hour exposure at 450K (350°F) the MA Al-Fe-Co alloys still exhibit a 7-24 MPa (1.0-3.5 ksi) gain in strength, while the MA Al-Li alloys are comparable to those for the unexposed material. The higher exposure temperature also resulted in a further slight reduction in ductility.

Elevated tensile tests on smooth bars, at 394K (250°F) and 450K (350°F) after 1000 hour exposures at 394K (250°F) and 450K (350°F), respectively, are also recorded in Table 6. Generally, the same strength stability after 1000 hour exposure, as noted above, were again observed. Strength decreases at the elevated temperatures, compared to room temperature properties, are of the same order as previously observed for unexposed materials.

The use of prealloyed powders for the higher alloy additions in the MA Al-Fe-Co system resulted in cleaner structures and higher hardness values (Figure 6) indicating that further strengthening had been obtained. The unexpectedly low strength levels observed were contradictory to the higher level of alloy additions used and the higher hardness values achieved. The

MA Al-Fe-Co alloys showed excellent stability of strength properties after long time exposure (Table 6). Short time strength losses were less than 20 percent when these alloys were tested at 394K (250°F) and less than 25 percent when testing was conducted at 450K (350°F). The same behavior was noted even after long time exposure at these elevated temperatures. Test results indicated that improvements in notched toughness, as measured by notched ratios, were obtained with the higher extrusion temperature, although the higher alloy content had a slight effect on toughness.

A comparison of two MA Al-Fe-Co alloys, both extruded at 700K (800°F) was made in an attempt to delineate the causes for the lower strength values currently observed. The results (Table 7) point out significant differences in addition level, powder source, dispersoid content, extrusion speed, and strain rate. Dispersoid level was intentionally kept low, within the program range, because of an observed brittleness during stress rupture testing of the MA Al-Fe-Co alloys in the earlier study. While this is possibly a contributing factor, it is believed that the principal cause for the lower strength values is the lower extrusion strain rate. A change in extruded bar shape (from round to rectangular) gave a lower extrusion ratio. This, coupled with a larger billet diameter and a lower ram speed, all contributed to a substantial reduction in strain rate. Another possible contributing, yet unknown factor, is the effect of prealloyed starting materials compared to the use of mixed powder elementals. While the use of prealloyed powder resulted in a much cleaner structure, the nature of the dispersoid obtained with prealloyed powders may be different from those obtained with elemental powders. X-ray examination, however, did not reveal any significant differences.

The MA Al-Li alloys showed substantially lower strength values than were anticipated, although significant improvements in ductility and notched toughness (Table 6) were obtained. An increase in dispersoid content (Lot 5A) gave approximately a 15 percent increase in strength properties. Mild hot working resulted in slight improvements in ductility and may prove beneficial for higher strength materials. On the other hand, an intermediate cold work improved strength levels and slightly reduced ductility. Neither the hot or cold working treatments had any significant effect on the excellent notched toughness values. Strength losses at elevated temperature were greater than those observed in the MA Al-Fe-Co alloys with an approximate 50 percent decrease occurring at 450K (350°F). Ductilities were observed to improve at the elevated temperatures. As with other mechanically alloyed materials, long time exposure at the elevated temperatures had no significant effect on the strength of the MA Al-Li alloys, either at room temperatures or at elevated temperatures.

A comparison between an MA Al-Li alloy previously evaluated[1] and a current material is shown in Table 7. Differences may be noted in alloy content, powder source, dispersoid level, and extrusion temperatures. It is believed that the higher extrusion temperature, coupled with the yet unexplained loss in Li content, are the primary factors influencing the lower properties.

TABLE 7. – EFFECT OF PROCESSING VARIATIONS ON PROPERTIES OF MA ALLOYS

	Al-1.7Fe-1.8Co LOT 8[A]	Al-4.1Fe-5.1Co LOT 1[B]	Al-1.9Li LOT 1[A]	Al-1.0Li LOT 5A[B]
POWDER SOURCE	100% ELEMENTAL	70% PREALLOYED Al-3Fe BALANCE ELEMENTALS	100% ELEMENTAL	100% PREALLOYED
DISPERSOID LEVEL, VOL.%	5.69	4.11	4.94	4.07
EXTRUSION TEMPERATURE, K (°F)	700 (800)	700 (800)	700 (800)	755 (900)
EXTRUSION RATIO	25.4:1	21.0:1	25.9:1	21.1:1
TIME AVERAGED STRAIN RATE, SEC^{-1}	3.26	0.71	1.67	1.19
AVERAGE RAM SPEED, CM/SEC	1.55	0.46	0.79	0.76
(IN/SEC)	(0.61)	(0.18)	(0.31)	(0.30)
HEAT TREATED HARDNESS, R_B[C][D]	65.5	73.5	79.0	55.0
TENSILE PROPERTIES AT RT				
YS, MPa (KSI)	394 (57.2)	360 (52.2)	472 (68.4)	278.5 (40.4)
UTS, MPa (KSI)	425 (61.6)	416 (60.4)	449 (81.1)	324.1 (47.0)
EL., %	5.0	5.0	2.5	12.0
RA, %	18.0	9.3	10.5	25.8
NOTCHED STRENGTH, MPa (KSI)	476 (69.1)	397 (57.6)	337 (48.9)	457.1 (66.3)
NOTCHED RATIOS - YIELD	1.21	1.10	0.71	1.64
UTS	1.12	0.95	0.60	1.41

NOTES:

(A) REFERENCE 1
(B) CURRENT STUDY
(C) ANNEALED 755K (900°F)/2 HOURS/ARGON/AC
(D) 783K (950°F)/90 MIN/AR/AC + 436K (325°F)/8 HRS/AIR/AC FOR LOT 1[A] ABOVE;
797K (975°F)/90 MIN/AR/WQ + 464K (375°F) 8 HR/AIR/AC FOR LOT 5A[B] ABOVE.

Powder Metallurgy (PM)

Notched Tensile Strength

The notched tensile results of the one and two step aged material, stretched 6 percent, is provided in Table 8. The notched tensile strength/yield strength versus yield strength correlation of PM 2618 and PM 2618 MOD B in Figure 13 provides a convenient method to indicate relative differences in toughness. The results indicate that NTS/YS ratio of the alloys in the NA temper is lower than in the underaged temper at the same strength. At the same strength, the NTS/YS ratio of PM 2618 MOD B is at the top of the scatter band for PM 2618 indicating that the dispersoid may be deleterious to toughness. However, this interpretation needs further examination since the degree of aging; i.e., the precipitate and dislocations interact, for alloy PM 2618 is different from that of PM 2618 MOD B at a similar strength. The ensuing toughness evaluation will test the artificially aged material at peak strength to assure the same dislocation-precipitate interaction. The initial increase in the NTS/YS ratio at the onset of artificial aging may be due to the precipitation of S' on dislocations leading to a reduction in the forest dislocation density. As the precipitate continues to grow the microstructure begins to lose its capacity to accommodate strain, thereby decreasing the NTS/YS ratio to a minimum at peak strength[17].

Table 9 is a listing of the high fracture toughness values of the PM 2124 and 2618 type alloys from the previous study measured by K_Q and an analysis using the 25 percent secant method[1]. The similarity between the NTS/YS values of the PM 2124 alloys and the present data suggests that similar toughness values are expected for PM 2618 and PM 2618 MOD B, Figure 14.

Fracture Toughness

The fracture toughness values of the high and low Mn containing 2124 alloys indicate that increasing the volume fraction of dispersoid reduces toughness. Optical fractography identifies the lower toughness specimen in the naturally aged condition by the larger area of plane strain fracture (optical macrograph), Figure 15. A difference is not optically observed between the artificially aged specimens. The 2618 type alloy possesses the lowest toughness of the three alloys, and displays the largest area of plane strain fracture in both tempers.

Observations by SEM as shown in Figure 15, reveals the different nature of fracture between the alloys PM 2618 MOD A, PM 2124 MOD, and PM 2124 in NA and AA tempers. Figure 15 (SEM 12X) shows the locally parallel arrangement of ridges and valleys of the fracture features. The source of this highly ordered arrangement is unknown. The aspect ratio and the occasional radial nature of features observed indicate the phenomenon is not related to the grain shape in the longitudinal or transverse section of the bar.

TABLE 8. – NOTCHED TENSILE TEST RESULTS OF SPECIMENS ONE AND TWO STEP AGED, STRETCHED 6%

PM HID 543 MOD				PM 2618				PM 2618 MOD B			
SINGLE STEP		DOUBLE STEP		SINGLE STEP		DOUBLE STEP		SINGLE STEP		DOUBLE STEP	
HOURS	NTS/YS	2ND STEP HRS.*	NTS/YS	HOURS	NTS/YS	2ND STEP HRS.*	NTS/YS	HOURS	NTS/YS	2ND STEP HRS.*	NTS/YS
436K (325°F)		PREAGE 24 HR 394K (250°F)		436K (325°F)		PREAGE 24 HR 394K (250°F)		436K (325°)		PREAGE 24 HR 394K (250°F)	
0	1.41	0	1.41	0	1.47	0	1.47	0	1.43	0	1.43
4	1.50	1	1.42	4	1.47	1	1.47	4	1.49	1	1.49
8	1.47	2	1.47	8	1.47	2	1.43	8	1.48	2	1.42
16	1.41	4	1.40	16	1.41	4	1.43	16	1.39	4	1.40
32	1.46	–	–	32	1.47	–	–	32	1.41	–	–
450K (350°F)		PREAGE 24 HR 408K (275°F)		450K (350°F)		PREAGE 24 HR 408K (275°F)		450K (350°F)		PREAGE 24 HR 408K (275°F)	
2	1.51	1	1.47	2	1.52	1	1.51	2	1.51	1	1.38
4	1.40	2	1.36	4	1.50	2	1.53	4	1.48	2	1.45
8	1.42	4	1.39	8	1.47	4	1.46	8	1.45	4	1.39
16	1.44	–	–	16	1.48	–	–	16	1.39	–	–
464K (375°F)		PREAGE 24 HR 422K (300°F)		464K (375°F)		PREAGE 24 HR 422K (300°F)		464K (375°F)		PREAGE 24 HR 422K (300°F)	
2	1.41	1	1.46	2	1.45	1	1.43	2	1.44	1	1.44
4	1.40	2	1.39	4	1.48	2	1.53	4	1.41	2	1.44
8	1.49	4	1.40	8	1.52	4	1.44	8	1.43	4	1.42
12	1.45	–	–	12	1.53	–	–	12	1.42	–	–

*AT 464K (375°F)

The tortuous fracture appearance of PM 2124 (0.5 wt. pct. Mn) relative to PM 2124 MOD (1.5 wt. pct. Mn) is shown in Figure 16. Closer examination in Figure 15 (SEM 1500X) indicates that the parallel fracture features in the artificially aged temper are more pronounced than in the naturally aged temper. Furthermore, the features are coarser in the 0.5 wt. pct. Mn alloy, PM 2124. The closer spacing of the ridges in the 1.5 wt. pct. Mn alloy, PM 2124 MOD, suggests that the advancing crack encounters less resistance to crack propagation than for PM 2124 during the test as a result of easier or more frequent void link-ups. Figure 15 (SEM 1500X) shows that the dimple size decreases at a given temper with the

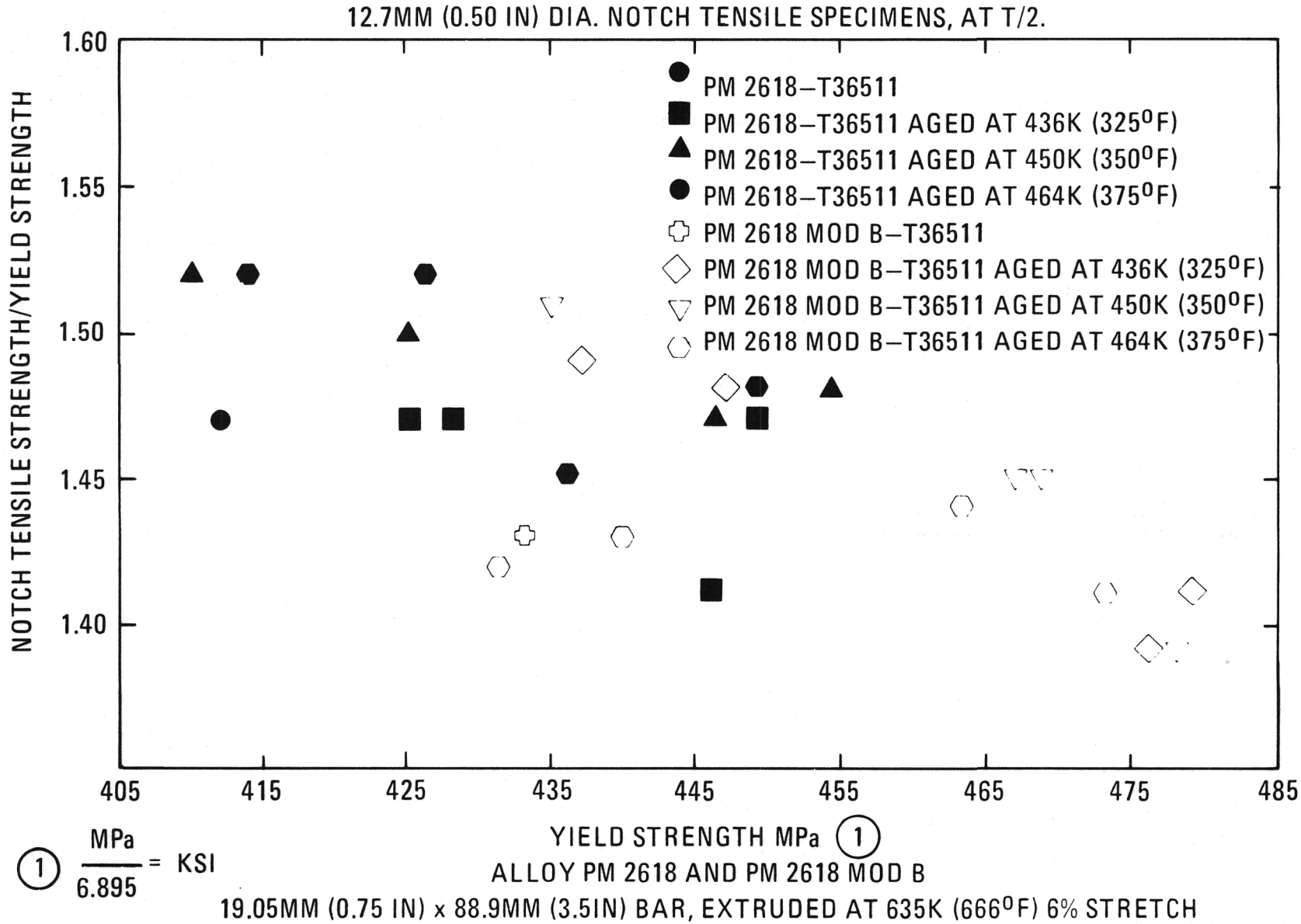

Figure 13. – The notched tensile strength/yield strength – yield strength correlation of PM 2618 and PM 2618 MOD B from the one step aging study.

TABLE 9. – THE K_Q AND R-CURVE DATA FOR DAMAGE TOLERANT ALLOYS

ALLOY	ORIENTATION	Y.S.,[8] MPa	Y.S.,[8] (KSI)	K_Q MPa $\sqrt{M}$	K_Q (KSI$\sqrt{IN.}$)	25% SECANT VALUE MPa $\sqrt{M}$	25% SECANT VALUE (KSI$\sqrt{IN.}$)
PM 2618 MOD A							
T3511	L-T	384	(55.7)	42.2	(38.4)[1, 3]	71.3	(64.9)
	T-L			43.5	(39.6)[1, 2, 3]	69.0	(62.8)
T36511	L-T	453	(65.7)	39.8	(36.2)[1, 3]	57.2	(52.4)
	T-L			46.7	(42.5)[1, 2, 3]	60.9	(55.4)
T8511[5]	L-T	407	(59.0)	41.0	(37.3)[1, 3]	55.7	(50.7)
	T-L			37.6	(34.3)[1, 3]	51.2	(46.6)
T86511[6]	L-T	452	(65.5)	31.9	(29.0)[3]	44.5	(40.5)
	T-L			33.0	(30.0) VALID K_{IC}	41.3	(37.6)
PM 2124 MOD							
T3511	L-T	420	(60.9)	44.6	(40.6)[1, 3, 4]	78.8	(71.7)
	T-L			49.6	(45.1)[1, 2, 3]	83.9	(76.4)
T36511	L-T	504	(73.1)	46.5	(42.3)[1, 3]	67.0	(61.0)
	T-L			54.3	(49.4)[1, 2, 3]	73.3	(66.7)
T8511[5]	L-T	410	(60.3)	53.0	(48.2)[1, 2, 3]	72.3	(65.8)
	T-L			50.8	(46.2)[1, 2, 3]	72.3	(65.8)
T86511[7]	L-T	493	(73.7)	40.7	(37.0)[3]	55.2	(50.2)
	T-L			42.9	(39.0)[1, 3]	57.0	(51.9)
PM 2124							
T3511	L-T	419	(60.8)	55.7	(56.7)[1, 2, 3]	100.2	(91.2)
	T-L			54.4	(49.5)[1, 2, 3]	98.2	(89.4)
T36511	L-T	515	(74.7)	57.7	(52.5)[1, 3]	95.5	(86.9)
	T-L			53.6	(48.8)[1, 2, 3]	100.2	(91.2)
T8511[5]	L-T	405	(58.7)	53.3	(48.5)[1, 2, 3]	91.9	(83.6)
	T-L			59.2	(53.9)[1, 2, 3]	90.5	(82.4)
T86511[7]	L-T	497	(72.1)	54.9	(50.0)[1, 3]	73.8	(67.2)
	T-L			56.4	(51.3)[1, 3]	79.8	(72.6)

NOTES:
1 – INVALID DUE TO INSUFFICIENT SPECIMEN THICKNESS
2 – INVALID DUE TO INSUFFICIENT FATIGUE PRECRACK LENGTH
3 – INVALID DUE TO $P_{MAX}/P_Q < 1.10$
4 – INVALID DUE TO CRACK FRONT CURVATURE EXCEEDING ALLOWED AMOUNT
5 – AGED 12 HR AT 464K (375°F)
6 – AGED 6 HR AT 464K (375°F)
7 – AGED 3 HR AT 464K (375°F)
8 – FROM AGING STUDIES PERFORMED IN PREVIOUS WORK (SEE NASA CONTRACTOR REPORT 1-65676)

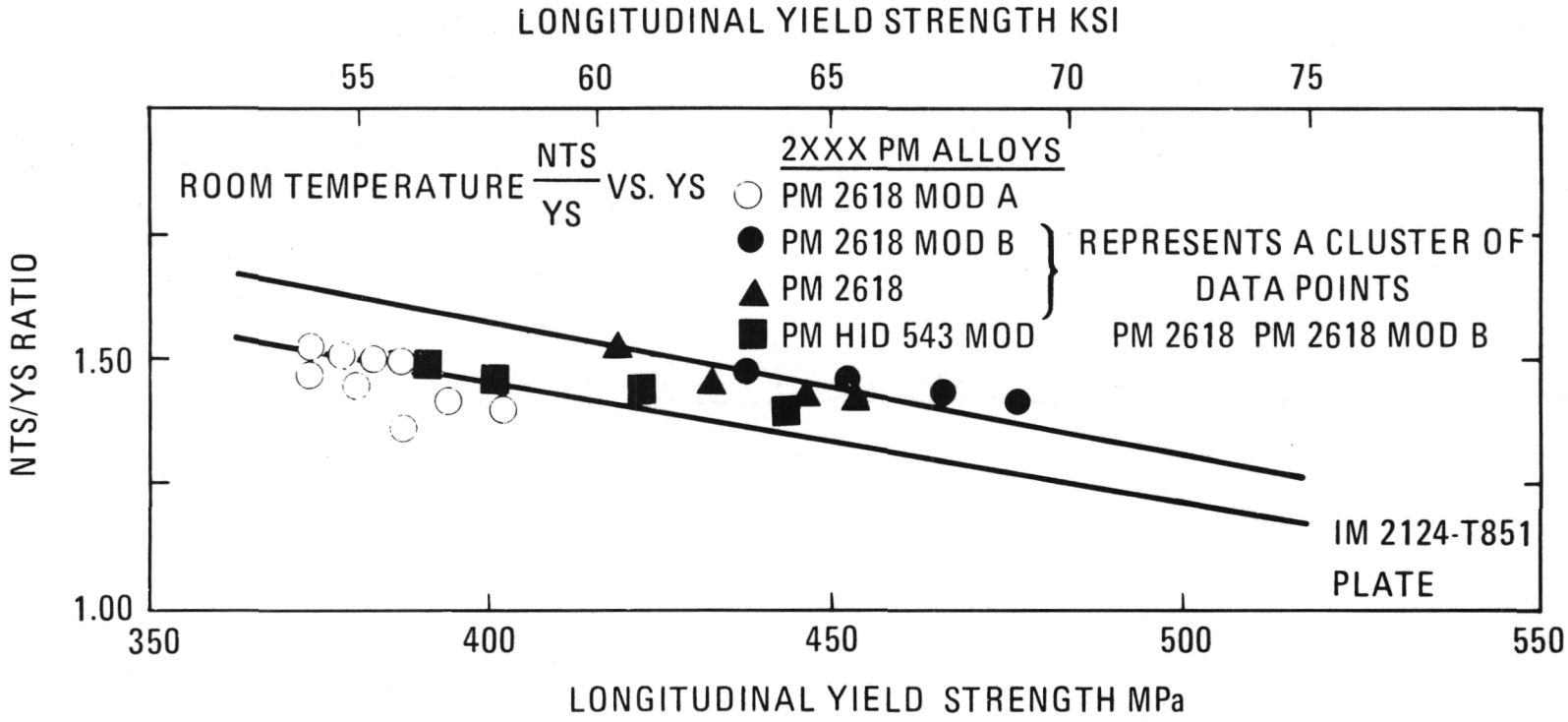

Figure 14. – NTS/YS correlation of alloys PM HID 543 MOD, PM 2618 and PM 2618 MOD B compared to IM and PM 2124-T851.

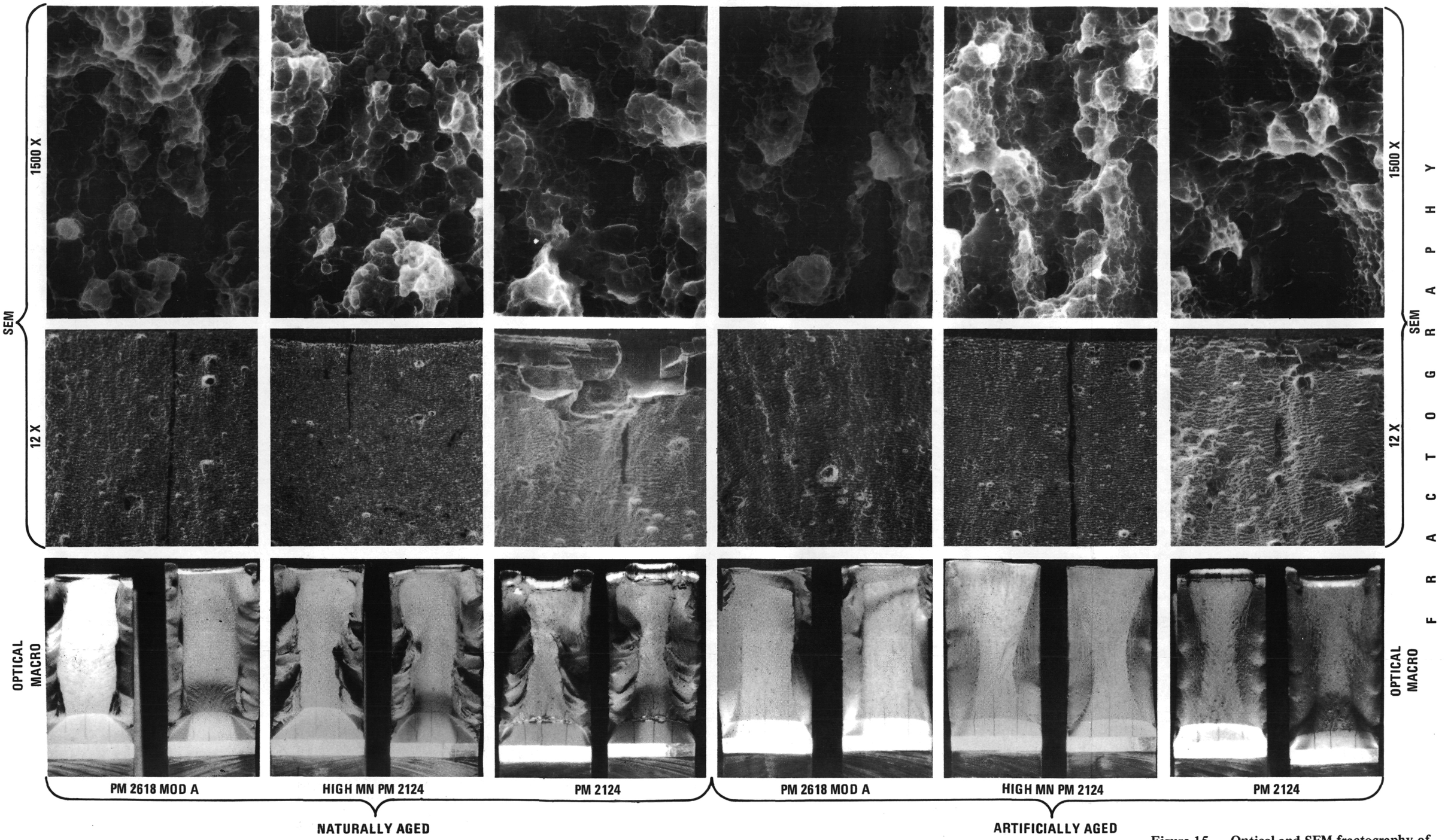

Figure 15. – Optical and SEM fractography of failed fracture toughness specimens.

Page Intentionally Left Blank

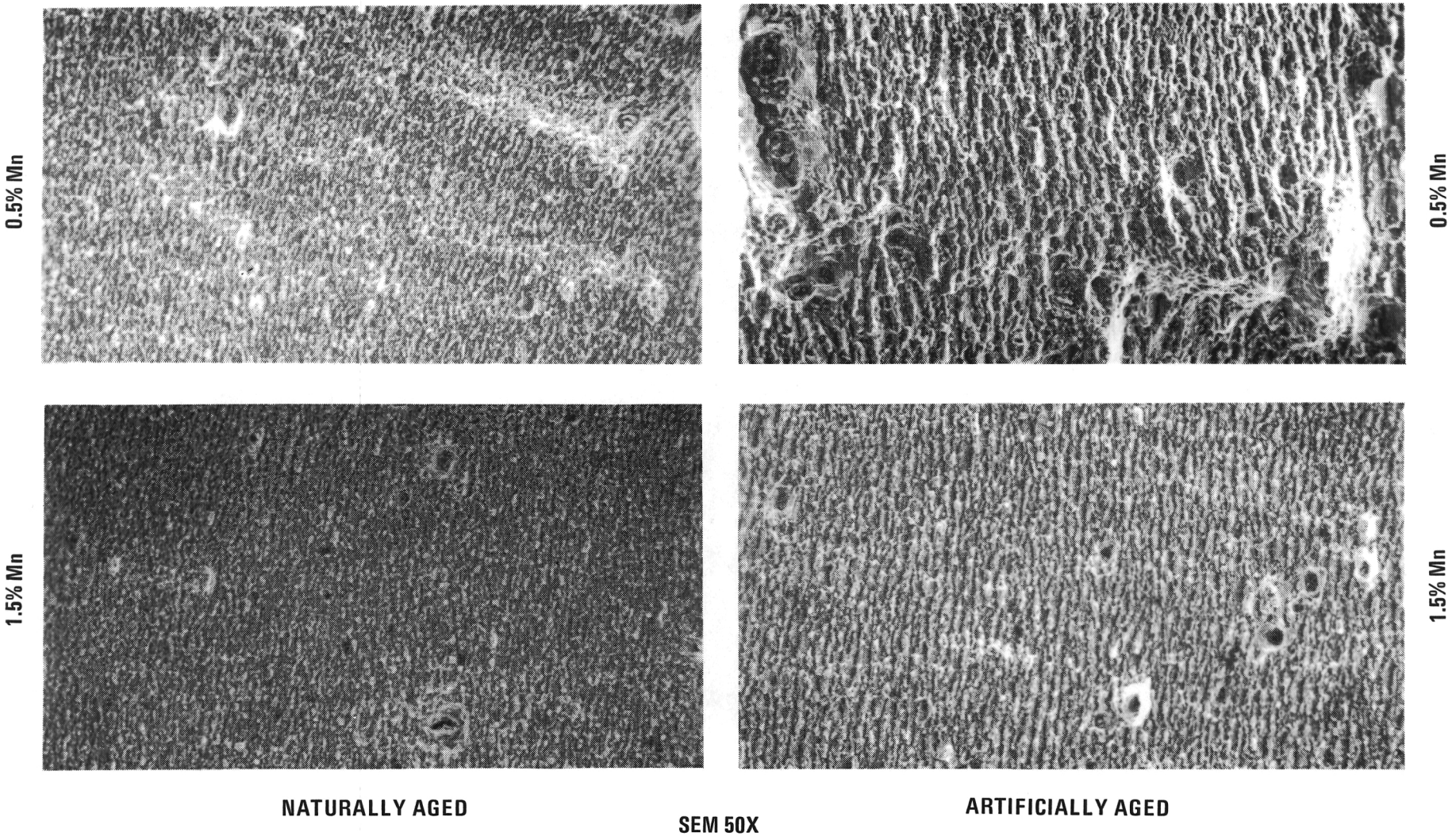

Figure 16. – SEM micrographs showing the difference in fracture appearance obtained by artificial aging and increasing the volume fraction of dispersoid.

increasing volume fraction of constituent: approximately 0.45 percent, 1.60 percent, and 2.40 percent for PM 2618 MOD A, PM 2124 MOD, and PM 2124, respectively[18]. The corresponding decrease in toughness associated with increasing the constituent volume fraction in the NA and AA temper is plotted in Figure 17. At a given constituent volume fraction the NA temper is tougher than the AA temper. The appearance of numerous, small closely spaced dimples in Figure 15 (SEM 1500X) are probably associated with the growth of large S and S' precipitates along the grain and subgrain boundaries in the AA temper[19]. Although portions of the specimen appear to have been fractured by a low energy absorbing intergranular fracture mode, the fine PM microstructure in the AA temper promotes good toughness.

Notched Fatigue Behavior

The initial property survey on PM 2XXX Al alloys revealed that PM 2124 type alloys are more fatigue resistant than conventionally processed IM 2124-T8511[1]. The magnitude of the improvement is temper dependent. In the AA temper alloys PM 2124 MOD and PM 2124 with 1.5 wt. pct. and 0.50 wt. pct. Mn, respectively, are slightly more fatigue resistant at 151 MPa (21.9 ksi). The cold worked AA temper further improves the fatigue strength over those of the conventionally stretched AA tempers. Although the improvement in fatigue resistance may be related to strength, compared to the IM 2124 control, the cold worked PM 2618 MOD A alloy in the AA temper is more fatigue resistant at a similar strength level. Alloy PM 2618 MOD A in the lower strength AA temper still displays slightly higher fatigue strength at 10^5 cycles than the IM control.

The greatest improvement in fatigue strength is obtained in the lower strength NA temper. The fatigue strengths of PM 2124 MOD and PM 2124 alloys are 39.3 percent and 23.3 percent greater than typical IM 2124-T8511 at 10^5 cycles. An increase in strength by cold rolling diminishes the fatigue strength relative to the -T3511 temper but still displays a significant increase in fatigue strength at 10^5 cycles as compared to the IM control.

The artificially aged tempers are not as fatigue resistant as the lower strength naturally aged tempers. The presence of S phase along the grain boundaries, accompanied by the large precipitation free zones (PFZ), may provide preferential crack initiation sites. Fatigue resistance is slightly improved by increasing the strength with the cold worked AA temper. Crack initiation is possibly delayed because of the material's greater strength, thus increasing the resistance to plastic strain at the notch tip. If the increase in strength is associated with the creation of a finer size and distribution of heterogeneously participated S' phase, an improvement in the homogeneity of deformation may be responsible for the improved fatigue resistance. The best fatigue resistance is observed for the naturally aged tempers. Microstructures consisting mostly of GP zones can accommodate greater amounts of strain as compared to the peak aged counterparts as indexed

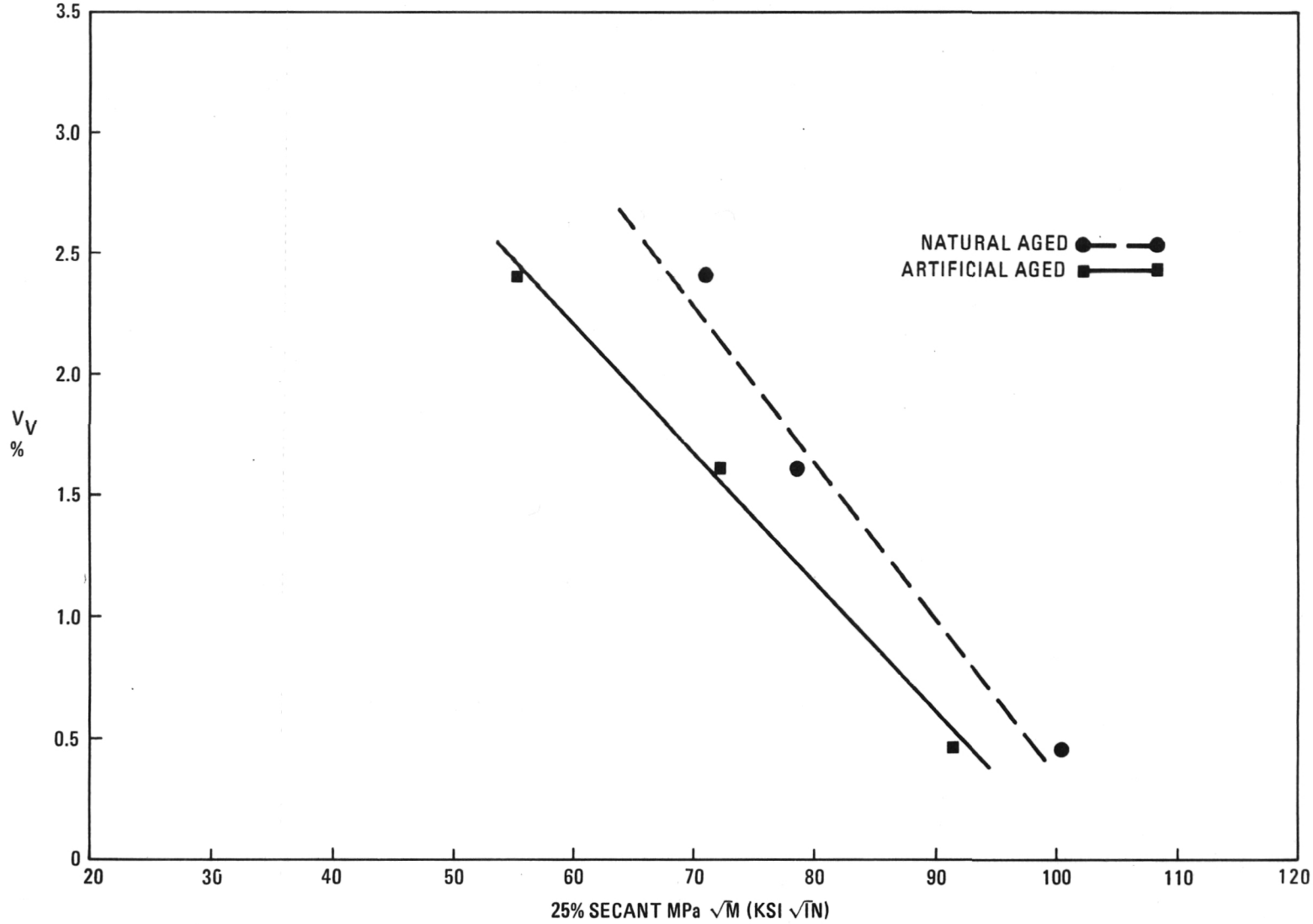

Figure 17. – Decrease in toughness with an increase in the volume fraction of dispersoid in alloys PM 2618 MOD A, PM 2124 HI MN, and PM 2124 in NA and AA tempers.

by the cyclic work hardening exponent[20], although the resistance to plastic strain at the notch tip is reduced. The loss in fatigue strength in the cold worked NA temper may be due to the diminished ability to accommodate strain as a consequence of the high dislocation density. Furthermore, the absence of large PFZ and grain boundary precipitates[1, 18] may eliminate crack initiation sites by reducing the differences in strength and deformation mode between the PFZ and matrix.

The degree of scatter in fatigue life at a given stress level is temper dependent. Assuming the fatigue crack growth rate (FCGR) of an alloy does not vary from environmental effects during the test, variations in total fatigue life at a given stress are created by differences in crack initiation times. If a material has an abundance of initiation sites, such as PFZs, large grain boundary precipitates, or a large volume fraction of intermetallic particles, initiation may occur at very reproducible times at these sites, and, therefore, contributes to lower scatter. For this reason, it is believed that a lower degree of scatter exists in the artificially aged tempers.

In the naturally aged tempers, a relatively large degree of scatter, characteristic of long life testing, exists at the 10^5 cycle regime. Implicit in the preceding hypothesis is that difficulty in crack initiation may cause greater scatter due to the smaller probability of a given constituent initiating a crack at the notch tip. The absence of the PFZs or S phases at the grain boundaries in the NA temper may be responsible for both the improved average fatigue strength and higher observed scatter. Other microstructural features may be responsible for initiation.

Figure 18 shows the variation in grain structure and second phase particle distribution between PM 2124-T3511 fatigue specimens displaying large differences in fatigue life; 53,400 and 170,900 cycles at 193.2 MPa (28 ksi). Pinhole X-ray patterns show no detectable differences in the type of texture, as shown in Figure 19. The coarse appearance of grain structures in Figure 18 with the lowest aspect ratio is more fatigue resistant than its finer counterpart possessing a larger aspect ratio. Relating the perpendicular grain dimension to the grain structure at the front and rear of the extrusion, Figure 7, indicates that the short life fatigue specimen is more closely associated with the rear of the extrusion. Figure 20 shows inclusions which are characteristically strung out along the rear of extrusions processed to a minimum billet length. The lower fatigue life may be due to the greater amount of inclusions at the rear portion since the finer grain structure is generally considered more crack initiation resistant[21].

An objective of the present research is to determine the effect of fine intermetallic particles on notched fatigue resistance in naturally and artificially aged tempers. The alloy selected is a variant of 2618 (similar to alloy PM 2618 MOD A (high Si, Fe, low Ni)). As a control, the same alloy without Fe and Ni is compared.

53,400 CYCLES AT 193.8 MPa (28 KSI)

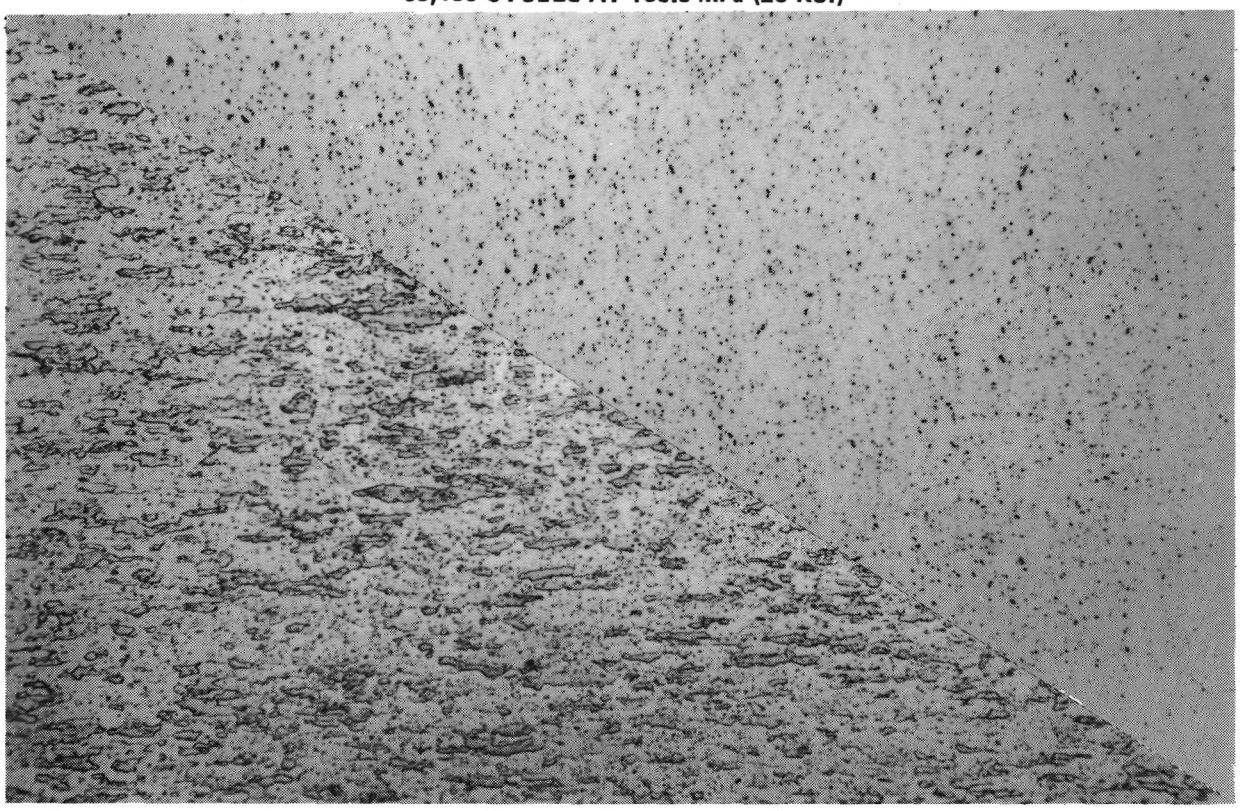

170,000 CYCLES AT 193.8 MPa (28 KSI)

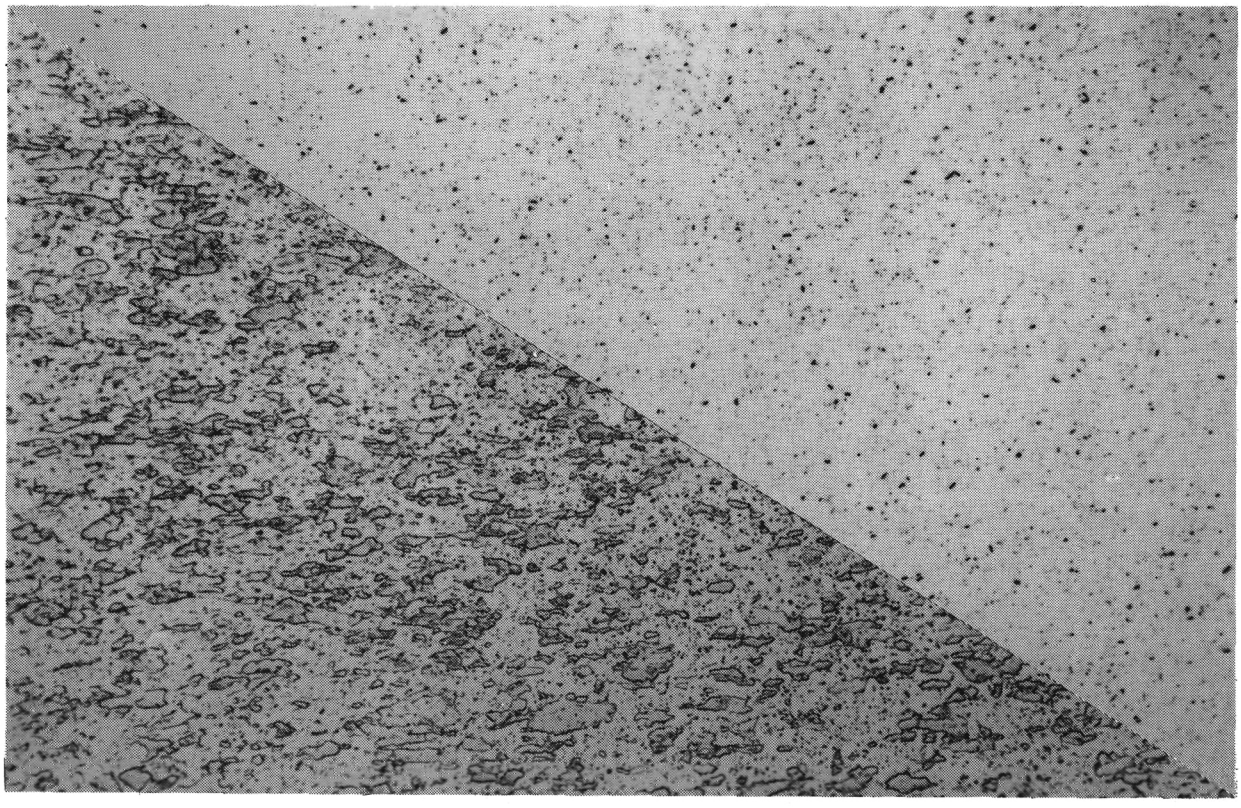

Figure 18. – Optical transverse section at 500X of naturally aged PM 2124 notched fatigue specimens fine (upper) and coarse grain structures with attendant second phase particle distributions.

(A)

53,900 CYCLES AT 193.8 MPa (28 Ksi)

(B)

170,900 CYCLES AT 153.8 MPa (28 Ksi)

Figure 19. – Pinhole x-ray pattern of notched fatigue specimens.

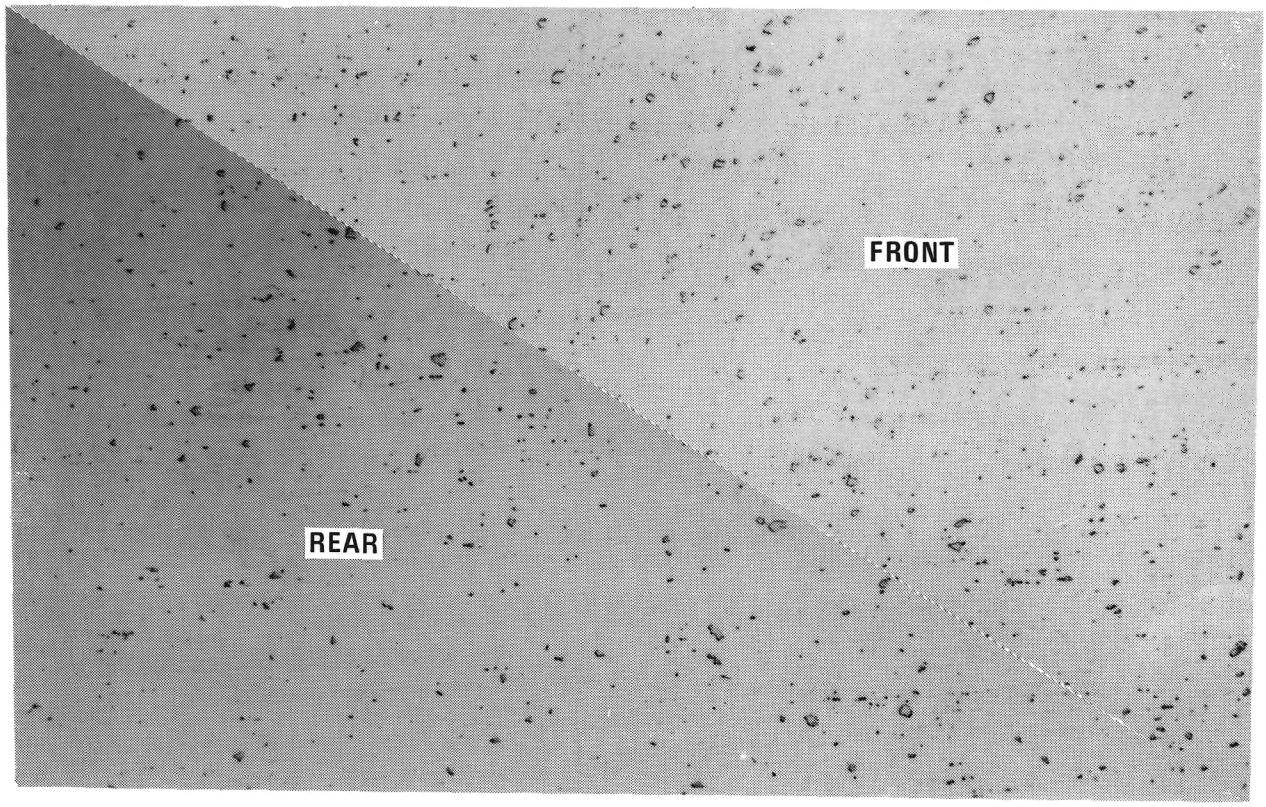

Figure 20. – Optical photomicrographs comparing strung out inclusions at front and rear of an extrusion processed to a minimum butt length.

Evidence exists to show that the dispersoid content influences fatigue resistance, hence the initiation resistance. Due to the fine dispersoid size, its influence on fatigue resistance is determined indirectly by the change in stress-life behavior. In the artificially aged temper, reducing the dispersoid content of PM 2124 MOD (high Mn) improved the fatigue resistance, particularly at 10^7 cycles. Conversely, in the naturally aged condition, reducing the dispersoid content decreased the fatigue resistance. Confirmation of the observed trend awaits the completion of fatigue tests comparing alloys PM 2618 and PM 2618 MOD B (no Fe or Ni).

The improved crack initiation resistance of PM 2124 in NA and AA tempers over that of conventionally processed IM 2124-T8511 is shown by SEM fractography, Figure 21. Crack initiation in the IM alloy occurs at points along the circumference of the notch, Figure 21. The cracks appear to grow radially (as indicated by the arrows) and link-up at interfaces (denoted by the heavy lines) to form a single crack front. Overload failure occurs in a circular region within the fatigue specimen. Similarly, crack initiation in the PM Al alloy, regardless of temper, occurs at points on the notch, Figure 22. Occasionally, initiation appears to have occurred along a segment of the circumference which appeared to advance linearly, Figure 22. Unlike IM Al alloys, overload always occurs at a region mostly adjacent to the notch tip, Figure 22. It is believed that the absence of continuous initiation around the circumference of the notch reflects the improved crack initiation resistance of PM processed material. The source of the variation in fatigue life of an alloy between different tempers and the cause of the high scatter observed in the naturally aged tempers was not observed by fractography.

Figure 21 shows that the initiation sites of the IM alloy are easily detected. Crack initiation in IM 2124-T4 was shown to occur at slip bands and large intermetallic particles at low stresses[22]. X-ray analyses at the initiation sites, however, were inconclusive in terms of identifying intermetallic particles. Figure 22 shows the initiation sites of PM 2124. Although the location of the initiation is obvious, specific microstructural features causing initiation in the PM 2124 alloys are more difficult to detect than its IM counterparts. The comparatively fine, uniform appearance of the fatigue surface did not allow positive identification of the crack initiation source. Inclusions or large intermetallic particles at the initiation sites were not detected by X-ray analysis.

Strain and stress controlled fatigue cracks initiate at grain boundaries in extruded PM X7091[23, 24]. Initiation sites in PM 2XXX Al alloys are presently unknown. Possible sites are suggested to include grain boundaries, and clusters of intermetallic particles, at the surface.

Figure 21. – Initiation sites, radial crack growth, interface link-ups (heavy lines) and overload surrounded by fatigue regions (upper photos) in ingot metallurgy 2124-T8511.

CONCLUSIONS

Mechanically Alloyed Powder Metallurgy (MAPM)

Al-Fe-Co Alloys

Strength and notched sensitivity at ambient temperature increase with a decrease in extrusion temperature.

MA Al-Fe-Co alloys exhibit good retention of strength and ductility properties after long time exposure (1000 hour) at 394K (250°F) and 450K (350°F).

At 394K (250°F), MA Al-Fe-Co alloys exhibit strength losses of less than 20 percent even after 1000 hour exposure. At 450K (350°F), strength losses of less than 25 percent were obtained, even after 1000 hour exposure.

The generally lower strength levels observed (in spite of improved hardness) is believed to be caused by the lower extrusion strain rates. This lower strain rate is due to the combined effects of changes in billet size (larger) and extrusion bar geometry (rectangular), coupled with a lower extrusion ratio and a reduced extrusion speed.

Prealloyed starting materials resulted in cleaner extruded bar structures. However, the use of prealloyed powders may affect the type of dispersoid formed which, in turn, may have an adverse (but as yet unknown) influence on strength.

Al-Li Alloys

A significant loss (as yet unexplained) in Li content, from 1.7 wt. pct. to approximately 1.0 wt. pct. was observed. This behavior, coupled with the higher extrusion temperature, is believed to contribute to the low strength levels.

An increase in dispersoid content resulted in a modest (approximately 15 percent) increase in strength, but with a slight decrease in ductility.

Excellent notched toughness and ductility properties were obtained in the MA Al-Li alloys. The notched toughness was not affected by subsequent hot or cold working procedures.

Hot working up to 25 percent reduction after extrusion had no significant effect on properties, yielding a mild increase in ductility combined with a slight strength reduction.

An intermediate cold work (up to 25 percent) improved strengths and slightly reduced ductility.

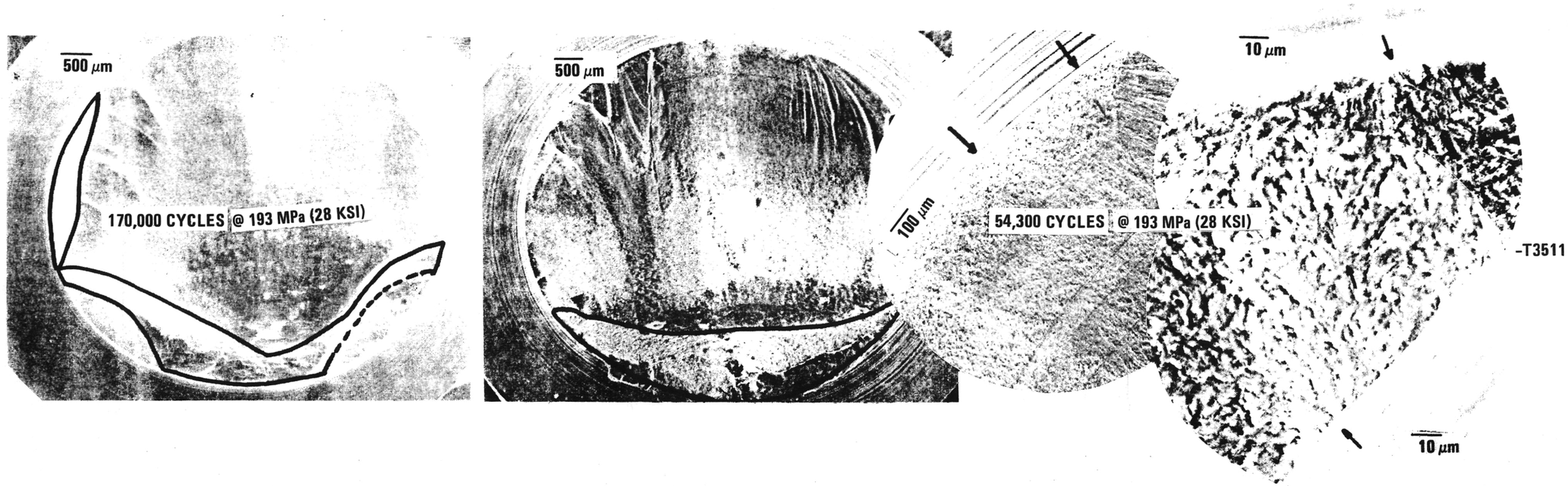

Figure 22. – SEM showing crack initiation, crack growth, overload, and fatigue regions for PM 2124 notched fatigue specimens.

Page Intentionally Left Blank

The MA Al-Li alloys retained approximately 75 percent of their strength after testing at 394K (250°F), but only 50 percent at 450K (350°F). Ductility improved as test temperatures were increased.

Long time exposure (1000 hour) at elevated temperatures had no significant effect on the strength/ductility properties of the MA Al-Li alloys.

Powder Metallurgy (PM)

The strength of the PM Al alloys is dependent on the solute content and amount of cold work applied prior to aging. The addition of Fe and Ni to the high Cu 2618 base composition is shown to reduce the yield strength in natural and artificial aged tempers. The loss in strength is attributed to the formation of the fine, uniformly distributed Al_7Cu_2Fe constituent, in lieu of strictly Al_9FeNi. The Mg modified PM 2219 alloy displayed the lowest strength of the alloys investigated, perhaps due to the low solution heat treatment temperature used.

An increase in the amount of cold work by stretching improves the naturally aged yield strength of the Fe and Ni free, high Cu 2618 alloy. In the artificially aged temper, the strength advantage is lost because of its lower solute content. An attempt to improve the strength by a two step aging treatment was unsuccessful.

The NTS/YS versus YS correlation of the high Cu PM 2618 alloys is similar to 0.5 wt. pct. Mn PM 2124 which exhibits a 10-15 percent improvement in toughness over IM 2124 at similar strengths. The lower NTS of the Mg modified 2219 is probably due to the coarse Al_2Cu particles which remain after solution heat treatment. Fractography of the PM 2124 precursors reveals that the decrease in toughness which results from increasing the dispersoid or constituent volume fraction by artificial aging is associated with a finer dimple size and spacing.

The improvement in fatigue resistance of IM 2124 obtained by PM processing is shown by SEM fractography, although microstructural constituents responsible for crack initiation were not detected. Optical metallography suggests that the large variation in the fatigue life in the naturally aged tempers is due to different specimen locations in the extrusion. The shortest fatigue life was associated with a finer grain structure and large amounts of inclusions observed at the rear of the extrusion as opposed to the front.

Contingent on results of elevated temperature testing and fracture toughness, the higher strengths of the initial PM 2124 and PM 2124 MOD (high Mn) alloys appear more promising than the most recently tested PM HID 543 MOD, PM 2618 MOD B and PM 2618 materials.

PLANNED FUTURE WORK

Mechanically Alloyed Powder Metallurgy (MAPM)

Further work on the mechanically alloyed PM metals is not presently planned. However, areas of needed work, as indicated by exploratory efforts to date, are delineated below for awareness purposes.

1. Emphasis in future work should be made to establish the effects of extrusion parameters (e.g., extrusion ratio, strain rate, bar geometry, etc.) on the properties of MA Al-Fe-Co alloys. An extensive structural analysis, including scanning electron and transmission electron microscopy is recommended, in conjunction with this study, to define the relationship of thermomechanical processing conditions to dispersoid formation and grain structure.

2. The choice of starting materials; i.e., prealloyed versus mixed elementals versus master alloys, warrants further examination to determine their contribution in terms of the type of dispersoid. This should be combined with a complete microstructural analysis.

3. The MA Al-Li system exhibits an excellent potential for low density alloys. The significant improvement in notched toughness, while possibly related to a lower Li content, warrants further examination of this system. A more extensive study of solution treatment and aging conditions, in conjunction with structural analysis, is also recommended.

4. While the attempt to mechanically alloy the Al-Fe-Ce alloy was unsuccessful, it is believed that a detailed evaluation of the attritor processing parameters required to produce MA Al-Fe-Ce alloys would be useful.

Powder Metallurgy (PM)

Areas of needed work are delineated below:

1. Obtain a better understanding of the equilibrium and metastable Al-Cu-Mg-Fe-Ni phase relationship in order to eliminate or minimize the loss of Cu to Fe- and Ni-rich constituents.

2. Re-evaluate the strength and notched tensile strength of the Al-Cu alloy, PM HID 543 MOD, in an optimum solution heat treated and aged condition. Evaluate the toughness, elevated temperature resistance, and notched fatigue strength at 10^5 cycles relative to the Al-Cu-Mg alloys.

3. Evaluate the effect of the Al_9FeNi and Al_7Cu_2Fe constituents in PM 2XXX Al alloys on elevated temperature stability, toughness, and notched fatigue behavior in the NA and AA tempers by means of a comparison of PM 2618 and PM 2618 MOD B.

4. Consider Zr, in lieu of or in addition to Mn, for elevated temperature stability improvement, and develop an improved understanding of elevated temperature strength behavior.

REFERENCES

1. Wald, G.G., "Supersonic Cruise Vehicle Technology Assessment, Study of an Over/Under Engine Concept - Advanced Aluminum Alloy Evaluation," NASA Contractor Report 165676, Contract Number: NAS1-14625, May 1981.

2. Brook, G.B., "Precipitation in Metals," Special Report No. 3, Fulmer Research Institute, 1965.

3. Wilson, R.N. and Forsyth, P.J.E., "Effects of Additions of 1% Iron and 1% Nickel on the Age Hardening Behavior of an Aluminum - 2.5% Copper - 1.2% Magnesium Alloy," J. Inst. Metals, Volume 94, page 8, 1966.

4. Armitage, W.K., "Influence on an Al-6 Wt. Percent Copper Clad Sheet Alloy of Small Additions of Magnesium," J. Inst. Metals, Volume 98, page 46, 1970.

5. Alcoa Technical Center, Unpublished data.

6. Wilson, R.N., Moore, D.M., and Forsyth, R.F.E., "Effects of 0.25% Silicon on Precipitation Processes in Aluminum - 2.5% Copper - 1.2% Magnesium Alloy," J. Inst. Metals, Volume 95, page 177, 1967.

7. Durand, D.P.H.A., Pelloux, R.M., and Grant, N.J., Materials Science and Engineering, Volume 23, pages 247-256, 1976.

8. Mondolfo, L.F., "Aluminum Alloys Structure and Properties," Butterworth, Inc.

9. Jones, W.R.D., and Das, P.P., "The Mechanical Properties of Aluminum - Lithium Alloys," Journal of the Institute of Metals, Volume 88, pages 435-443, 1959-60.

10. Alcoa Technical Center, Unpublished data.

11. Chadwick, R., "The Hot Extrusion of Non-Ferrous Metals," Metallurgical Reviews, Volume 4, pages 189-255, 1959.

12. Muntz, A., Zangril, A., and Metzger, M., Metallurgical Transactions, Volume 11A, pages 1863-1968, November 1980.

13. Alcoa Technical Center, Unpublished data.

14. Dieter, G.E., "Mechanical Metallurgy," McGraw Hill Book Company, Second Edition.

15. Cook, J.D., and Notting, J., "The Mechanisms of Phase Transformations in Crystalline Solids," Proceeding of an International Symposium by Inst. Met. Univ. Manchester, Session II, pages 54-59, July 1968.

16. Vnuggink, J.E., Aluminum, Volume 49, pages 601-605, 1973.

17. Garrett, G.E. and Knott, J.F., Metallurgical Transactions, Volume 9A, pages 1187-1201, September 1978.

18. Petit, J.I., "Thesis on the Structure and Properties of Three Powder Metallurgically Processed Al-Cu-Mg Alloys," MIT, October 1980.

19. Kenman, I., Metallurgical Transactions A, Volume 2A, pages 1761-1770, July 1971.

20. Sanders, R.E., Jr., and Starke, E.A., Jr., Materials Science and Engineering 2B, pages 53-68, 1977.

21. Starke, E.A., Jr., and Lutjering, G., Fatigue and Microstructure, ASM Material Science Seminar, St. Louis, Missouri, October 14-15, 1978.

22. Kung, C.Y., and Fine, M.E., Met. Trans., Volume 10A, pages 603-610, May 1979.

23. Walker, J.A., "Thesis on the Microstructure and Properties of Extruded CT91-T7X151," Georgia Institute of Technology, December 1980.

24. Kuo, V., Personal Communications, Georgia Institute of Technology.

1. Report No.	2. Government Accession No.	3. Recipient's Catalog No.
NASA CR-165965		

4. Title and Subtitle	5. Report Date
DEVELOPMENT OF POWDER METALLURGY AL ALLOYS FOR HIGH TEMPERATURE AIRCRAFT STRUCTURAL APPLICATIONS - PHASE II	30 November 1982
	6. Performing Organization Code
7. Author(s)	8. Performing Organization Report No.
D.J. Chellman	LR 30364
	10. Work Unit No.
9. Performing Organization Name and Address	
Lockheed-California Co. P.O. Box 551 Burbank, CA 91520	11. Contract or Grant No. NAS1-16048, Mod 1 and 2
	13. Type of Report and Period Covered
12. Sponsoring Agency Name and Address	16 July 1980-15 August 1981
National Aeronautics and Space Administration Washington, D.C. 20546	14. Sponsoring Agency Code

15. Supplementary Notes

NASA Technical Monitors S.M. Dollyhigh and W.B. Lisagor

16. Abstract

This report describes the analytical and test work completed by the Lockheed-California Company during FY 1980/1981 on the exploratory work being conducted on advanced powder metallurgy Al alloys in support of the NASA supersonic cruise research project. The FY 1980/1981 development effort is a continuing study and covers two types of Al powder metallurgy systems. The development of mechanically alloyed heat resistant Al alloys for aircraft was directed toward higher strength targets and higher service temperatures. The use of higher alloy additions to MA Al-Fe-Co alloys, employment of prealloyed starting materials, and higher extrusion temperatures were investigated. While the MA Al-Fe-Co alloys exhibited good retention of strength and ductility properties at elevated temperatures and excellent stability of properties after 1000 hour exposure at elevated temperatures, a sensitivity of this system to low extrusion strain rates adversely affected the level of strength achieved. MA alloys in the Al-Li family showed excellent notched toughness and property stability after long time exposures at elevated temperatures. A loss of Li during processing and the higher extrusion temperature 482K (900°F) resulted in low mechanical strengths. Subsequent hot and cold working of the MA Al-Li had only a mild influence on properties. The advantage of using prealloyed powders as a starting material, while producing cleaner structure, could not be clearly established because of the attritor processing anomalies encountered and because of the changes in thermo-mechanical processing conditions. Attempts to mechanically alloy the Al-Fe-Ce alloy

17. Key Words (Suggested by Author(s))	18. Distribution Statement
High Temperature Al Alloys Powder Metallurgy Mechanical Alloying Rapid Solidification Technology High Strength-Corrosion Resistant Damage Tolerant-Fatigue Resistant Alloy Development	Unclassified - Unlimited

19. Security Classif. (of this report)	20. Security Classif. (of this page)	21. No. of Pages	22. Price
UNCLASSIFIED	UNCLASSIFIED	73	

For sale by the National Technical Information Service, Springfield, Virginia 22161

16. Abstract (Continued)

were unsuccessful. A greater in-depth study of processing parameters will be required to establish appropriate attritor conditions.

Six powder metallurgy extruded materials were studied during FY 1980/1981. PM 2618 MOD A (high Si, Fe, low Ni), PM 2124 MOD (high Mn) and PM 2124, which were tested and reported in previous work, received follow-on optical, scanning electron microscopy, and pinhole X-ray metallographic evaluations. The Alcoa atomization/compaction/consolidation/extrusion sequence was used to produce the new test materials; PM Hiduminium (HID) 543 MOD (low Cu), PM 2618, and PM 2618 MOD B (no Fe, Ni). The promise of elevated temperature property improvement based on published data was the basis for selecting these three new alloys. Composition, X-ray crystallographic, optical metallographic, and thermomechanical precipitation strengthening studies were conducted for the new materials. Ambient property comparisons were made for the six materials of this project and they were further compared with other ingot and powder metallurgy members of the 2XXX Al alloy family.